MEASUREMENT OF TRANSPORT PROPERTIES OF POLYACRYLIC SYSTEMS USING A GRAVIMETRIC SORPTION METHOD

By

Yılmaz YÜREKLİ

A Dissertation Submitted to the
Graduate School in Partial Fulfillment of the
Requirements for the Degree of

MASTER OF SCIENCE

Department: Chemical Engineering
Major: Chemical Engineering

İzmir Institute of Technology
İzmir, Turkey

September, 2003

ACKNOWLEDGEMENT

The present research was performed between 2001 and 2003. Most of the investigations were carried out in the laboratories of Chemical Engineering in İzmir Institute of Technology. The financial supports of Izmir Institute of Technology Research Fund accountancy (2001 Müh 16) and TUBİTAK (Misag-144) are gratefully acknowledged.

I wish to give my thanks to the supervisors: Assoc. Prof. Sacide Alsoy Altınkaya, Prof. Devrim Balköse and Asst. Prof. Funda Tıhmınlıoğlu for their valuable advice, help and support during the course of this research.

The researchers, experts and anyone who lightened my way of research from Chemical Engineering Department of İzmir Institute of Technology, Prof. David Venerus who has measured loss modulus and storage modulus of copolymer samples from Illinois Institute of Technology, Prof. Surva Mallapragado who has performed NMR analysis of the copolymer sample from Iowa State University, and Dr. John Zielinksi who has given valuable discussion and orientation from Air Products Inc., USA, are highly appreciated.

I also present my deepest thanks to Organik Kimya A.Ş. for supplying the polymer samples and Dr Guia Kaslowski for helpful suggestion from the same company.

I would like to appreciate deeply my friends Mehmet Gönen, Metin Becer, Burcu Alp, Sevdiye Atakul, Hacer Yenal, Serdar Öztürk, and Özge Topçuoğlu for their friendship and encouragements.

Finally, my thanks go to my family and my wife Hanife Yürekli for her help, and appreciations during performing experiments and the writing of this thesis.

Izmir, September 2003

Yılmaz Yürekli

ABSTRACT

In this study, transport properties of methyl methacrylate (MMA) monomer in methylmethacrylate–butylacrylate copolymer were measured using a gravimetric sorption technique. This copolymer is used as a binder in indoor and outdoor paint formulation. Following the application of the paint material, residual monomers (volatile organic compounds, VOC) are emitted over time. Thus, it is important to understand and determine emission characteristics of residual monomers in order to evaluate their impact on the indoor air quality. With the growing awareness of the problems associated with the indoor air quality, there is now strong pressure for manufacturing, and selecting paint materials as well as other building materials with low VOC emissions. Success in both manufacturing and choosing environmentally friendly building materials is greatly facilitated by the availability of mathematical models for predicting the emission rates of VOCs from these materials. Emission rates of monomers, VOCs, from paint and other building materials are primarily governed by the diffusion within the material. The key parameter required to predict emission rates is the diffusion coefficient of monomers within the polymer. In addition, the knowledge of diffusivity of monomers in the polymer is prerequisite in the design of a devolatilization unit to produce paint materials with reduced monomer contents. In accordance with these concerns, the second objective of this study was to derive a physical model to predict the emission characteristics of the MMA from the paint material using experimentally determined diffusivity and solubility data.

As a first step in the experimental study, MMA-BA copolymer sample was characterized to determine its glass transition temperature, degradation temperature, functional groups and composition using thermal analysis, fourier transform infrared spectroscopy and nuclear magnetic resonance analysis techniques. Samples were provided by Organic Kimya A.Ş. in the form of an emulsion and films were prepared using a film applicator. Final characterization of the samples was done by observing microstructure of the films and measuring the thickness using a scanning electron microscope.

Diffusivity and solubilities were measured over a temperature range of 40 ^{o}C to 60 ^{o}C by a new type of gravimetric sorption apparatus called magnetic suspension balance. In order to determine concentration dependence of the diffusivities, monomer temperature was increased with small step changes. Diffusivity of MMA in MMA-BA

copolymer varied in the range of $1x10^{-8}$ -$1x10^{-7}$ cm^2/s as the weight fraction of MMA increased from 0.03 to 0.2.

The most popular theory derived by Vrentas and Duda was successfully used to correlate the diffusivity data of the MMA as a function of temperature and concentration. The free volume parameters were obtained by rheological measurements and with the use of limited diffusion data. Based on these parameters, the predictive ability of the model was found to be satisfactory. The solubility data were accurately modeled by Flory Huggins thermodynamic theory. The Flory Huggins interaction parameter determined as 0.726 indicated that MMA cannot completely dissolve the copolymer. According to the prediction of this theory, maximum amount of MMA which can be absorbed in the copolymer is around 53 % by volume.

In the second part of this study, the physical model derived was used to predict MMA concentration in air under different conditions. Model predictions have shown that increasing air exchange rate significantly reduce the concentration of MMA in air. If the exchange rate is not changed, increasing air velocity or temperature causes an increase in MMA concentration in air. In all cases, at long emission times concentration of MMA in the paint material does not change significantly indicating that transport of MMA is controlled by diffusion in the paint material.

ÖZ

Bu çalışmada, ağırlık ölçümüne dayalı sorpsiyon tekniği kullanılarak metil metakrilat (MMA) monomerinin metilmetakrilat-bütilakrilat kopolimeri içerisindeki transport özellikleri ölçülmüştür. Bu kopolimer iç ve dış cephe boya formülasyonunda bağlayıcı madde olarak kullanılmaktadır. Boyanın uygulanmasının akabinde, içinde kalan artık monomerler (uçucu organik bileşenler) zamanla dış ortama yayılırlar. Bu sebeple, boyadaki monomerlerin oda içerisindeki havanın kalitesi üzerinde olan etkilerini incelemek için bu monomerlerin yayılma karakteristiklerinin bilinmesi ve belirlenmesi önemlidir. Günümüzde iç mekanlarda monomerin solunması ile birlikte artan problemlerin farkına varılmasıyla, diğer yapı malzemelerinde olduğu gibi düşük miktarda uçucu organik bileşikleri içeren boyaların üretimi ve seçimi yönünde güçlü bir baskı vardır. Çevre dostu yapı malzemelerinin hem üretimi hem de seçiminde başarıyı yakalamak, uçucu organik bileşenlerin bu maddelerden dış ortama geçiş hızlarını hesap etmede kullanılabilecek matematiksel modellerin varlığıyla büyük ölçüde kolaylaşmıştır. Monomerlerin veya diğer uçucu organik bileşenlerin boyadan ve diğer yapı malzemelerinden dış ortama geçiş hızları, esas itibari ile malzeme içerisindeki difüzyon tarafından kontrol edilir. Bu nedenle geçiş hızlarını doğru tahmin etmede gerekli olan en önemli parametre monomerin polimer içerisindeki difüzyon katsayısıdır. Buna ilaveten, artık monomer içeriği azaltılmış boya üretiminde kullanılan saflaştırma ünitesinin tasarımı için de monomerlerin polimer içerisindeki difüzyon katsayısını bilmek şarttır. Bu konularla bağlantılı olarak bu çalışmanın ikinci amacı, MMA monomerinin boyadan dış ortama geçiş hızını etkileyen parametreleri tanımlayacak fiziksel bir matematik modelin türetilmesi ve deneysel olarak ölçülmüş difüzyon ve çözünürlük verilerinin bu model içinde kullanılmasıdır.

Deneysel çalışmada ilk adım olarak, MMA-BA kopolimer örneği camsı geçiş sıcaklığı, bozunma sıcaklığı, fonksiyonel grupları ve kompozisyonunun belirlenmesi için termal analiz, fourier transform kızıl ötesi spektroskopisi ve nükleer manyetik rezonans analizi teknikleri kullanılarak karakterize edilmiştir. Kullanılan kopolimer örneği Organik Kimya A.Ş. tarafından emülsiyon formunda gönderilmiş, bu emülsiyonlardan film aplikatörü kullanılarak farklı kalınlıkta filmler hazırlanmıştır. Örneklerin son karakterizasyonu filmlerin mikro yapıları gözlemlenerek ve kalınlıkları taramalı elektron mikroskopunda ölçülerek yapılmıştır.

Difüzyon katsayıları ve çözünürlükler manyetik askılı terazi adı verilen yeni tip bir ağırlık ölçümüne dayalı sorpsiyon cihazı kullanılarak 40 ^{o}C'den 60 ^{o}C'ye uzanan sıcaklık aralığında ölçülmüştür. Difüzyon katsayılarının konsantrasyona bağımlılığını belirlemek amacıyla, monomer sıcaklığı küçük adım aralıklarıyla arttırılmıştır. MMA'ın MMA-BA kopolimeri içerindeki difüzyon katsayısı MMA'ın ağırlık kesri 0.03'ten 0.2'ye arttığında $1x10^{-8}$-$1x10^{-7}$ cm^2/ s aralığında değişmiştir.

MMA'ın difüzyon katsayısının sıcaklık ve konsantrasyona göre değişimini veren korelasyon Vrentas ve Duda tarafından geliştirilmiş olan free volume teorisi kullanılarak elde edilmiştir. Free volume parametreleri reolojik ölçümler ve sınırlı sayıdaki difüzyon verisi kullanılarak elde edilmiştir. Bu parametrelere dayanarak elde edilen korelasyonun farklı sıcaklıktaki difüzyon katsayılarını doğru tahmin ettiği bulunmuştur. Çözünürlük verileri Flory-Huggins termodinamik teorisi kullanılarak modellenmiştir. 0.726 olarak belirlenen Flory-Huggins etkileşim parametresi MMA'ın kopolimeri tamamiyle çözemeyeceğini göstermiştir. Bu teoriden, kopolimerce absorbe edilebilecek maksimum MMA miktarı hacimce % 53 olarak hesaplanmıştır.

Bu çalışmanın ikinci kısmında, türetilen fiziksel model farklı koşullar altında havanın içerisindeki MMA konsantrasyonunu hesaplamak için kullanılmıştır. Simülasyon sonuçları, artan hava değişim hızının hava içerisindeki MMA konsantrasyonunu önemli ölçüde azalttığını göstermiştir. Eğer havalandırma sıklığı değiştirilmezse, artan hava hızı veya sıcaklığının hava içerisindeki MMA'ın konsantrasyonunda bir artışa sebep olacağı görülmüştür. Bütün koşullar altında , uzun sürelerin sonunda boya içerisindeki MMA konsantrasyonu önemli ölçüde değişmemektedir. Bu durum MMA'ın transportunun, boya malzemesi içerisindeki difüzyon tarafından kontrol edildiğine işaret etmektedir.

NOMENCLATURE

F	rate of transfer per unit area of section ($g/cm^2.s$)
C	the concentration of diffusing substance (g/cm^3)
X	space coordinate measured normal to the section (cm)
D	diffusion coefficient (cm^2/s)
T	time (s)
M_t	the total amount of vapor absorbed by the polymer film at time t (g)
M_∞	the equilibrium sorption attained theoretically after infinite time (g)
L	thickness of the polymer film (cm)
$(DEB)_D$	Deborah number
θ_D	the characteristic time of the diffusion process (s)
D^*	diffusion coefficient, which is an appropriate measure of the diffusional transport in the system (cm^2/s)
D_0	constant preexponential factor (cm^2/s)
$\hat{V}_1^*$	the specific critical hole free volume of solvent required for a jump (cm^3/g)
$\hat{V}_{FH}$	the average hole free volume per gram of the mixture (cm^3/g)
K_{11}	solvent free-volume parameter ($cm^3/g.K$)
K_{21}	solvent free-volume parameter (K)
K_{12}	polymer free-volume parameter ($cm^3/g.K$)
K_{22}	polymer free-volume parameter (K)
T_{g1}	glass transition temperature of the solvent (K)
E	energy per mole that a molecule needs to overcome attractive forces which hold it to its neighbours (J/mol.K)
1	solvent
2	polymer
A_1	constant
M_1	molecular weight of the solvent (g/mol)
$\hat{V}_c$	molar volume of the solvent at its critical temperature (cm^3/mol)
$\hat{V}_1^0$	specific volume of pure solvent (the inverse of the density) at the temperature of interest. (cm^3/g)

P_1	vapor pressure of solvent at T (atm)
P_1^0	saturation vapor pressure of solvent (atm)
$\hat{V}_1^0(0)$	molar volume of the equilibrium liquid solvent at 0°K (cm^3/mol)
k	proportionality constant
N_A	avogadro's number
R	gas constant
C_1 and C_2	WLF constants
G^M	Molar Gibbs free energy
n_s	Moles of solvent
a	Activity
C_a	Concentration of monomer in air
X	Thickness of the film at any time (cm)
k_1^G	Mass transfer coefficient of monomer
P_{1i}^G	Partial pressure of monomer at paint-air interface
P_{1b}^G	Partial pressure of monomer in air
$\dot{m}_1$	Amount of monomer diffused from paint to air (g/s)
V	Volume of room (m^3)
Q	Air exchange rate (m^3/h)
S_{MP}	The mass of balance reading (g)
m_{vac}	The mass of balance reading at vacuum(g)

Greek Letters

λ_m	the characteristic time of the fluid (s)
ω_1, ω_2	mass fractions of solvent and polymer
γ	overlap factor for free volume
ξ	ratio of the critical molar volume of the solvent jumping unit to the critical molar volume of the polymer jumping unit
ϕ_1	volume fraction of the solvent in the polymer
μ_1	Chemical potential of solvent
η	Viscosity (g/cm-s)

ρ_1	Concentration of monomer in the paint
ρ_{vapor}	Vapor density of monomer (g/cm^3)

TABLE OF CONTENTS

LIST OF FIGURES

LIST OF TABLES

CHAPTER 1

INTRODUCTION

Acrylic copolymers are widely used in paint industry due to their wide range of colors, outstanding optical clarity, and excellent ultraviolet resistance. Incomplete polymerization of the monomers, impurities in the monomers and undesirable secondary reactions occurring during the synthesis lead to residual volatile organic compounds (VOC) in the finished product. When paint is applied on the surface, these compounds emit into the atmosphere over time, which change indoor air quality, and cause general symptoms, such as headache, eye, nose, or throat irritations, dry cough, dizziness and tiredness. With the growing awareness of the problems, there is a strong pressure for manufacturing and selecting paint materials with low VOC emissions. The volatile residues are usually removed by vacuum or steam stripping of a polymer melt or of polymer particles in a devolatilizer where the process is controlled by diffusion of these residues in the polymer. Success in choosing environmentally friendly paints depends on predicting the emission rates of VOCs from the paint, which are primarily controlled by diffusion within the paint. Consequently, design and optimization of the devolatilization process as well as determining the VOC emission characteristics of the paints require knowledge of the diffusion rate of monomer or other residues in the polymer.

The main objective of this study is to measure diffusivity and solubility of methylmethacrylate monomer in poly(methylmethacrylate-n-butylacrylate). The copolymer is manufactured by Organic Kimya A.Ş., Turkey and is used as a binder in indoor/outdoor paint formulation. Measurements were carried out at different temperatures and concentrations using a new type of gravimetric sorption equipment called magnetic suspension balance. A correlation that describes diffusivity of methylmethacrylate in the copolymer as a function of temperature and concentration was obtained using Vrentas and Duda (1977a) free volume theory and its predictive ability was tested. In addition, the solubility data were correlated by Flory Huggins theory (Flory 1953).

Another objective of the study is to derive a mathematical model to predict emission rate of methylmethacrylate from the copolymer. Two kinds of mathematical

models are available in the literature for predicting the rate of VOC emission. The first kind of these models is the empirical model which is based on fitting an appropriate mathematical expression to a set of experimental data (Matthews et al., 1987; Christianson et al., 1993). Although empirical models are simple and easy to use, they do not provide insight into physical emission mechanisms. Thus, they are not suitable for other conditions and systems. Physical models focus on the VOC mass transfer principle. Some of these physical models considers only surface effects (Dunn and Tichenor, 1988; Axley, 1991; Clausen et al., 1991; Tichenor et al., 1991) while other physical models assume that the rate of emission is only controlled by internal diffusion (Dunn, 1987; Dunn and Chen, 1992; Little et al., 1994).

In this study, the model derived by Alsoy (1998) for predicting drying behavior of solvent coated polymer films was extended to determine emission characteristics of MMA from the copolymer into air. According to this model, the rate of emission is controlled both by diffusion in the polymer and evaporation from the surface. In addition, diffusivity of VOC in the polymer is not assumed constant which is the case in all models available in the literature. Key parameters required in the model are diffusivity and solubility correlations, both of which were obtained from experimental measurements. In order to predict methylmethacrylate concentration in air for various conditions, model equations were solved numerically.

CHAPTER 2

DIFFUSION AND THERMODYNAMICS OF POLYMER-SOLVENT SYSTEMS

2.1. Free Volume Concepts

The motion of molecules within a liquid, relative to one another and with respect to stationary reference points is greatly affected by temperature, pressure and composition of the fluid. This microscopic motion influences macroscopic properties, which can be determined with simple experiments. Viscosity and diffusivity are among these measurable properties. Diffusion characteristics of polymer-solvent systems are different than those of low molecular weight mixtures due to complicated chain like structure of polymers. As the temperature is raised, kinetic energy of the polymer chains increases causing the material to expand and enhancing the available free volume. This expansion of volume not only facilitates reorientational motion and migration of species through the material but it also reduces the friction between polymer chains during flow.

The free volume theory of transport provides a useful method for predicting and correlating mutual-diffusion coefficient above and below the glass transition of the polymer solvent system. The basic free volume concept was first proposed by Cohen and Turnbull (1959), and modified by Fujita (1961), and redefined by Vrentas and Duda (1977a) for both mutual and self-diffusion in polymer solvent system.

2.2. Vrentas and Duda Free Volume Theory

In Vrentas and Duda free volume theory, the volume of a liquid can be divided into two groups, occupied volume by the molecules, and unoccupied volume (free volume) between the molecules. As two molecules come closer to each other, the repulsive forces cannot be negligible, so all the free volume within a system is not equally accessible for molecular transport. Due to usual random thermal fluctuations some of this free volume is continuously being redistributed and is called as hole free

volume, since molecular transport takes place in this part of the free volume. As it is seen from the Figure 2.1, the remaining part of the free volume, which is not being continuously redistributed and also is not available for molecular migration, is called as interstitial free volume. According to Vrentas and Duda free volume theory, a molecule

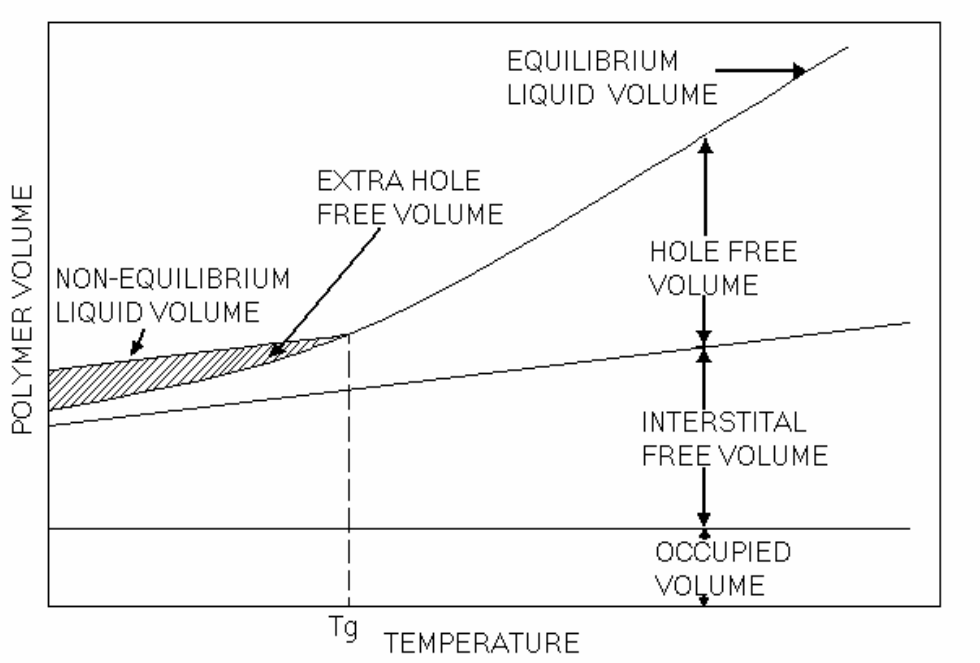

can migrate if it has enough energy to overcome attractive forces by the nearest neighbor and if there is a sufficient size of hole free volume.

Assuming that the vacancy and energy availabilities can be represented by the Boltzmann probability functions, the expression for solvent self-diffusion (D_1) is given as follows; (Vrentas and Duda 1977b)

$$D_1 = D_0 \exp\left[\frac{-E}{RT}\right] \exp\left[\frac{-\left(\omega_1 \hat{V}_1^* + \omega_2 \xi \hat{V}_2^*\right)}{\frac{\hat{V}_{FH}}{\gamma}}\right] \qquad (2.1)$$

The total hole free volume available for diffusion $\hat{V}_{FH}/\gamma$, has contributions from both the solvent and the polymer as shown below;

Figure 2.1.Characteristics of the volume of a polymer above and below the glass transition temperature (T_g)

$$\frac{\hat{V}_{FH}}{\gamma} = \frac{K_{11}}{\gamma}\omega_1\left(K_{21} + T - T_{g1}\right) + \frac{K_{12}}{\gamma}\omega_2\left(K_{22} + T - T_{g2}\right) \tag{2.2}$$

Self diffusion coefficients measure the mobility of each species in a homogenous mixture. Polymer-solvent systems are usually exposed to conditions that impose concentration gradients. The effects of the imposed gradient on molecular motion are characterized by mutual-diffusion coefficient (D). For the case of polymer-solvent solutions, D can be written as follows (Vrentas and Duda 1977c):

$$D = \frac{D_1\omega_1\omega_2}{RT}\left(\frac{\partial\mu_1}{\partial\omega_1}\right)_{T,P} \tag{2.3}$$

Using Flory-Huggins thermodynamic theory to calculate chemical potential gradient, $\left(\partial\mu_1/\partial\omega_1\right)$, D can be represented by Equation 2.4

$$D = D_1\left(1-\phi_1\right)^2\left(1-2\chi\phi_1\right) \tag{2.4}$$

When the penetrant concentration, ω_1 is below the value of 0.9 then the activation energy, E, is constant and hence Equation 2.1 is modified as given below.

$$D_1 = D_0^* \exp\left[\frac{-\left(\omega_1\hat{V}_1^* + \omega_2\xi\hat{V}_2^*\right)}{\frac{\hat{V}_{FH}}{\gamma}}\right] \tag{2.5}$$

where,

$$D_0^* = D_0 \exp\left[\frac{-E}{RT}\right] \tag{2.6}$$

2.3. Estimation of Free Volume Parameters

The concentration and temperature variations of diffusion coefficient for a polymer-solvent system can be determined from Equation 2.1, if the density-temperature data, viscosity-temperature data for pure polymer and pure solvent, if three

or more values of polymer-solvent diffusivity data at two or more temperatures, and if thermodynamic data such as sorption equilibrium data for a polymer-solvent system are available.

To evaluate the parameters in Equation 2.1, following procedures can be proceeded.

i) $\hat{V}_1^*$ and $\hat{V}_2^*$:

They are estimated by equating them to equilibrium liquid volumes at 0°K. Molar volumes at 0°K can be estimated using group contribution method developed by Sugden and Biltz, and Haward (1970) have summarized these methods.

$$\hat{V}_1^* = \hat{V}_1^0(0) \tag{2.7}$$

$$\hat{V}_2^* = \hat{V}_2^0(0) \tag{2.8}$$

ii) $\frac{K_{11}}{\gamma}, K_{21} - T_{g1}$:

These two parameters can be easily evaluated if viscosity of the solvent is available over a wide temperature range. The relationship between the viscosity of the solvent and its free volume parameters are given by the following expression (Vrentas and Duda, 1998)

$$\ln \eta_1 = \ln A_1 + \frac{\gamma \hat{V}_1^* / K_{11}}{K_{21} - T_{g1} + T} \tag{2.9}$$

iii) $\frac{K_{12}}{\gamma}, K_{22} - T_{g2}$:

The free volume parameters of the polymer can also be evaluated if the viscosity of the polymer measured at glass transition temperature and 100°C above the glass transition temperature. However, viscosity data near the glassy region are usually not

available. $\frac{K_{12}}{\gamma}$ and $K_{22} - T_{g2}$ are obtained from Williams, Landel and Ferry parameters (WLF parameters), C_1, C_2 using following expressions.

$$K_{22} = (C_2^g)_2 \tag{2.10}$$

$$\frac{\gamma \hat{V}_2^*}{K_{12}} = 2.303(C_1^g)_1(C_2^g)_2 \tag{2.11}$$

An extensive list of polymer WLF parameters has been published by Ferry (1970). When these constants are not available for the polymer of interest, then they are obtained from experimental measurements of shift factor at different temperatures. The relationship between the shift factor and the temperature is given by the following equation.

$$\log a_T = -\frac{C_1(T - T_{ref})}{C_2 + T - T_{ref})} \tag{2.12}$$

Shift factor can be obtained by superimposing dynamic mechanical measurements (loss modulus, G', and storage modulus, G'' as a function of frequency) at different temperatures.

iv) D_0^*, ξ :

ξ is a key parameter in free volume theory which is defined as the ratio of solvent to polymer jump size units. They are obtained by fitting at least 3 experimental polymer-solvent diffusivity data to Equation 2.1.

2.4. Flory-Huggins Theory

At the end of the sorption process the number of solvent molecules moving from vapor phase to polymer phase is the same as the number of solvent molecules moving in the other direction. When there is no net flow between the two phases, the chemical

potential of the solvent in each phase is the same. This is the definition of true equilibrium

$$\mu_{penetrant}^{Vapor} = \mu_{penetrant}^{Polymer} \tag{2.13}$$

The definition of chemical potential difference is given as follows:

$$\frac{\Delta\mu_i}{RT} = \frac{\partial}{\partial n_i}\left(\frac{\Delta G^M}{RT}\right)_{n_{j,j\neq i}} \tag{2.14}$$

The equation for the free energy of polymer solutions was derived independently and almost simultaneously by Flory and Huggins and uses many of the assumptions of regular solution theory.

$$\frac{\Delta G^M}{RT} = n_S \ln\phi_S + n_P \ln\phi_P + n_S\phi_P\chi \tag{2.15}$$

The first two terms on the right hand side of Equation 2.15 is combinatorial entropy and the symbols ϕ_S and ϕ_P represent the volume fractions of the solvent and the polymer respectively. The third term uses the parameter χ to describe the interactions between the components and it is related to the change in energy when solvent/solvent and polymer/polymer contacts. Flory and Huggins assumed that the polymer has flexible chain of segments and that each of segments is equal in size to a solvent molecule. According Flory Huggins theory, the chemical potential difference is given as follows (Flory, 1953):

$$\frac{\mu_S - \mu_S^0}{RT} = \ln(1-\phi_P) + (1-\frac{1}{M})\phi_P + \phi_P^2\chi \tag{2.16}$$

In this equation, the number of chain segment, M is very large and the second term on the right hand side of Equation 2.16 can be written as only polymer volume fraction, ϕ_P.

If the chemical potential is expressed in terms of activity, then Equation 2.13 can be rewritten as follows:

$$\mu_s^{o,Vapor} + RT \ln a_s^{Vapor} = \mu_s^{o,Polymer} + RT \ln a_s^{Polymer} \tag{2.17}$$

Furthermore, if the same reference state is chosen for both vapor and polymer phase, then equilibrium condition be redefined as follows:

$$\ln a_s^{Vapor} = \ln a_s^{Polymer} \tag{2.18}$$

2.5. Estimation of Flory-Huggins Interaction Parameter

The interaction parameter χ, can be determined from the solubility data in which equilibrium weight fraction of solvent in the polymer is known as a function of the solvent vapor pressure P_1 using Flory-Huggins equation:

$$Activity = \frac{P_1}{P_1^0} = \phi_1 \exp\left(\phi_2 + \chi \phi_2^2\right) \tag{2.19}$$

χ parameter is regressed from Equation 2.19 by minimizing the difference between the experimental and theoretical activities.

CHAPTER 3

MODELING OF SORPTION PROCESS

3.1. Basic Equations

Diffusion is the process by which matter is transported from one part of a system to another as a result of random molecular motions. Mutual diffusion coefficients are used to describe diffusion in solutions under the influence of concentration gradients, whereas a self-diffusion coefficient is an indication of the rate at which a concentration gradient of a labeled species is dissipated in an otherwise uniform solution. Fick (1855) has found an expression for diffusion on a quantitative basis by adopting the mathematical equation of heat conduction derived by Fourier. The mathematical theory of diffusion in isotropic substances is therefore based on the hypothesis that the rate of transfer of diffusing substance through unit area of a section is proportional to the concentration gradient measured normal to the section;

$$F = -D\frac{\partial C}{\partial x} \tag{3.1}$$

It must be emphasized that the statement expressed mathematically by Equation 3.1 is in general consistent only for an isotropic medium, whose structure and diffusion properties in the neighbourhood of any point are the same relative to all directions. Because of this symmetry the flow of diffusing substance at any point is along the normal to the surface of constant concentration through the point.

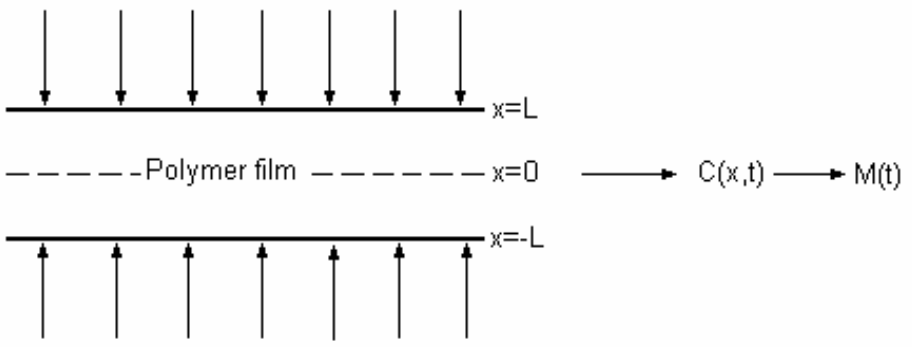

Figure 3.1. Schematic view of sorption process

3.2. Modeling of Sorption Process

During a typical differential sorption experiment, a polymer sample with a thickness of 2L is exposed to penetrant from both sides as shown in Figure 3.1. The weight gain or loss is recorded as a function of time. In order to determine diffusivity of penetrant in the polymer film, unsteady state sorption process is modeled using following assumptions:

1. The diffusion process is isothermal and the effect of pressure on the liquid density is negligible.
2. The vapor phase is essentially pure, and the liquid phase is a binary mixture of penetrant and polymer
3. There are no chemical reactions in the liquid phase
4. Diffusion process is a viscous Fickian process
5. For all times during the sorption experiment, there is an equilibrium at the phase interface because of the instant equilibration of the phase boundary in the step change sorption experiment.
6. In the rectangular geometry, the diffusion process is a one dimensional transport process in a polymer film of thickness 2L.
7. For convenience, the mutual diffusion coefficient D is assumed to be independent of concentration because of small step change of solvent vapor pressure.

Under these assumptions, sorption process is described by the following equation.

$$\frac{\partial C}{\partial t} = D\frac{\partial^2 C}{\partial x^2} \tag{3.2}$$

Initially the concentration of the penetrant in the polymer is uniform,

$$t=0 \rightarrow C= C_0 \tag{3.3}$$

At times t>0, concentration of the penetrant at the surfaces is constant and equal to its equilibrium concentration

$$t>0 \rightarrow x= \pm L \quad C=C_{eq} \tag{3.4}$$

Analytical solution of Equation 3.2 through 3.4 is given by Crank (1975).

$$C(x,t) = -\frac{2C_0}{\pi}\sum_{n=1}^{\infty}\frac{1}{n}((-1)^n - 1)\sin\left(\frac{n\pi}{L}\right)xe^{-\left(\frac{n\pi}{L}\right)^2 Dt} \tag{3.5}$$

Integration of Equation 3.5 from x=-L to x=+L provides an expression for the dimensionless uptake as follows;

$$\frac{M_t'}{M_\infty'} = \frac{M_t - M_0}{M_\infty - M_0} = 1 - \frac{8}{\pi^2}\sum_{m=0}^{\infty}\frac{1}{(2m+1)^2}\exp\left\{-D(2m+1)^2\pi^2 t/4L^2\right\} \tag{3.6}$$

Crank (1975) has shown that at short times as t $\rightarrow$0, Equation 3.6 can be simplified as follows.

$$\frac{M_t'}{M_\infty'} = \frac{2}{\sqrt{\pi}}\left(\frac{Dt}{L^2}\right)^{1/2} \tag{3.7}$$

Equation 3.7 indicates that at short times, uptake curve becomes linear and diffusion coefficient can be easily calculated from the slope of the plot of M_t'/M_∞' vs. $t^{1/2}$.

3.3. Typical Sorption Kinetics

Results of the typical sorption experiments are usually presented by plots of M_t'/M_∞' as a function of square root of time ($t^{1/2}$). Sorption kinetics is categorized according to the shape of these plots.

3.3.1. Fickian Sorption

If diffusional transport for a step change differential sorption experiment is described by the classical theory of diffusion, then it is usually stated that the sorption curves (plots M_t' / M_∞' vs. $t^{1/2}$) should exhibit the following behavior.

1. In the initial stages of the sorption process, the sorption curve is linear.
2. The sorption curve is always concave with respect to the $t^{1/2}$ axis above the linear portion
3. The sorption curves for all values of the film thickness 2L will form a single curve when plotted as M_t' / M_∞' versus $t^{1/2}$ /2L for fixed initial and final penetrant concentrations.
4. The sorption and desorption curves at the same temperatures are superimposed.

It is generally assumed that solvent diffusion in rubbery polymers is a Fickian diffusion process (Vrentas & Vrentas 1998).

3.3.2. Two Stage Sorption

Two-stage sorption is frequently defined as anomalous sorption and it consists of 2 different parts: a) fast Fickian sorption, b) slow Non-Fickian sorption. The sorption curve is Fickian from the start until it starts to level off. However, instead of reaching the saturation level typical for Fickian sorption, the curve is extended through a non-Fickian part. Finally, saturation level is reached.

3.3.3. Sigmoidal Sorption

Sigmoidal sorption curves are S-shaped, showing a point of inflection. This type of curve is observed due to non-Fickian diffusion behavior or due to show establishment of the equilibrium at the surface of the film.

3.3.4. Case II Sorption

Case II sorption is another form of the non-Fickian diffusion. Typical uptake curve in case II sorption follows a linear kinetics, ie., when M_t / M_∞ is plotted against time.

Diffusion coefficient of the polymer-solvent system following CaseII Sorption was calculated using the sorption or desorption curve based on the simplified Crank equation.

3.4. Diffusion Regimes

The nature of the diffusion process is simply determined by calculating a dimensionless group called as Deborah, $(DEB)_D$, which is defined as the ratio of two characteristic times, relaxation time for the polymer-solvent system (λ_m) and the characteristic diffusion time (θ_D).

$$(DEB)_D = \frac{\lambda_m}{\theta_D} \tag{3.8}$$

θ_D is proportional to square of the film thickness, thus, $(DEB)_D$ is proportional to L^{-2}. When $(DEB)_D << 1$, the characteristic relaxation time is smaller than the diffusion time and the diffusion process is said to be viscous Fickian diffusion. When the diffusion Deborah number is sufficiently large, there is a negligible time variation of the polymer structure during the diffusion process. This type of diffusional transport can be denoted as elastic Fickian diffusion. Vrentas &Duda (1977b) have proposed that diffusional transport for large Deborah number can be satisfactorily described by the classical theory of diffusion even though the system is not a purely viscous fluid mixture. When the Deborah number is order of unity, the molecular relaxation and the diffusive transport process occur in comparable time scales and rearrangement of polymer chains and movements of solvent molecules take place simultaneously. This type of diffusional transport is denoted as viscoelastic (anomalous) nonFickian diffusion.

Vrentas et.al (1996) have concluded the regime of diffusion processes such that for viscous Fickian diffusion $(DEB)_D < 10^{-2}$, for elastic Fickian diffusion $(DEB)_D > 10^2$, and for anomalous nonFickian diffusion $10^{-2} < (DEB)_D < 10^2$. For the cases of viscous Fickian and elastic Fickian diffusion, the sorption curves (M_t' / M_∞' versus $t^{1/2}$ /L) for films of different thicknesses give a single curve means that the binary mutual diffusion coefficient of the polymer-solvent system is independent of L. However for the case of anomalous, nonFickian diffusion, the sorption curve for films of different thicknesses may not yield a single curve as is required by the equations of classical theory. As a result the apparent values of the mutual diffusion coefficient D may depend on L.

CHAPTER 4

MODELING OF VOLATILE ORGANIC COMPOUND (VOC) EMISSION AND CONCENTRATION IN BUILDINGS

A variety of building materials such as paints, carpets, furniture can act as a source of volatile organic compound (VOC). After they are installed or applied, residual quantities of VOC in these materials are emitted over time. These compounds cause many negative effects on human health such as headache, tiredness, eye, nose, or throat irritations, dry cough and dizziness. (Kim et al., 2001; Meininghaus et al., 1999; Molhave, 1989; US EPA, 1990; WHO, 1989; Yang, 1999). Thus, it is important to determine the emission characteristics of these materials based on a predictive mathematical model. For this purpose, the drying model derived by Alsoy (1998) was extended to predict concentration of volatile organic compound both in air and in the coating material.

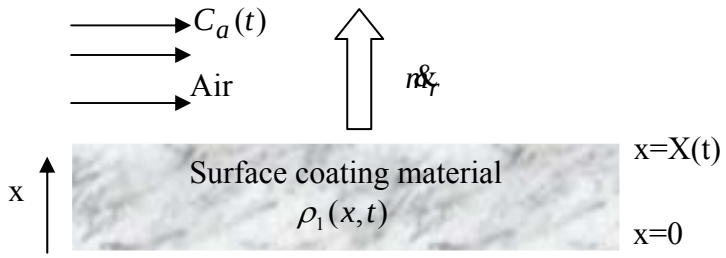

Figure 4.1. Schematic view of the monomer diffusion from surface coating materials to air.

The model considers the geometry shown in Figure 4.1. Surface coating material having an initial thickness of L contains VOC with an initial concentration of ρ_{1_0} . The system is treated as a pseudobinary system and it is assumed that VOC diffuses only through "x" direction. This is a reasonable assumption since the thickness of the coating material is much smaller compared to its other dimensions. In addition, diffusion of VOC in the coating material is assumed "Fickian" type and temperature gradient in the

coating material due to evaporation of VOC is negligible. Also, model assumes that the room temperature is maintained constant. Under these assumptions, the concentration of VOC in the coating material as well as the thickness of the coating material are given by similar equations derived for drying of solvent coated polymeric films by Alsoy (1998). Thus, these equations were adapted as follows:

Species continuity equation for VOC:

$$\frac{\partial \rho_1}{\partial t} = \frac{\partial}{\partial x}\left(D \frac{\partial \rho_1}{\partial x} \right) \tag{4.1}$$

The decrease of thickness of the paint film due to evaporation of VOC, dX/dt, is given by Equation 4.2.

$$\frac{dX}{dt} = -\left[\frac{-D \frac{\partial \rho_1}{\partial x} \hat{V}_1}{(1 - \sum_{i=1}^{N-1} \rho_1 \hat{V}_1)} \right] \tag{4.2}$$

Initial and boundary conditions required for the solution of Equation 4.1 are described as follows:

at t=0 $$\rho_1(0, x) = \rho_{1o} \tag{4.3}$$

$$x = 0 \qquad \frac{\partial \rho_1}{\partial x} = 0 \tag{4.4}$$

$$x = X(t) \qquad -\left(D \frac{\partial \rho_1}{\partial x} \right) - \rho_1 \frac{dX}{dt} = k_1^G (P_{1i}^G - P_{1b}^G) \tag{4.5}$$

In the case of drying of solvent coated polymer films, the concentration of the solvent in the bulk phase, P_{1b}^{G}, is kept constant since the process is continuous. However, this is not the case when VOC is emitted into air, i.e., due to accumulation and/or depletion of VOC, P_{1b}^{G} changes with time. To determine time rate of change of concentration of MMA in air, Equation 4.6. was added.

$$V\frac{dC_a}{dt} = \dot{m}_r - QC_a \tag{4.6}$$

where the relationship between the concentration of VOC in air C_a, and P_{1b}^{G} is given by ideal gas law.

$$P_{1b}^{G} = C_a RT \tag{4.7}$$

and the rate of emission of VOC, $\dot{m}_r$, is described as follows:

$$\dot{m}_r = k_1^G A(P_{1i}^G - P_{1b}^G) \tag{4.8}$$

CHAPTER 5

EXPERIMENTAL DEVICES FOR THE MEASUREMENT OF DIFFUSIVITIES IN POLYMER-SOLVENT SYSTEMS

Many techniques have been investigated for the measurement of diffusivity of polymer solvent systems such as inverse gas chromatography, (Pawlisch 1987), piezoelectric crystal (Saby-Dubreuil 2001), gravimetric (McDowell 1998, Vrentas et al., 1984) and volumetric sorption techniques.

5.1. Inverse Gas Chromatography (IGC)

In a typical application, the polymer is used as the stationary phase in a chromatographic column. The solute is vaporised and injected into a carrier gas flowing through the column. As the solute is swept through the column, it can interact with the polymer via absorption. Thermal conductivity detector (TCD) or flame ionization detector (FID) at the end of the column detects the molecules passing through the column and gives a chromatogram with respect to time. Figure 5.1 shows the experimental set-up of finite concentration inverse gas chromatography. The retention time of the solute and the shape of the elution profile (ie., chromatographic peak) reflect the strength and nature of the interactions that occur between the polymer and the solute and can be used to study those interactions.

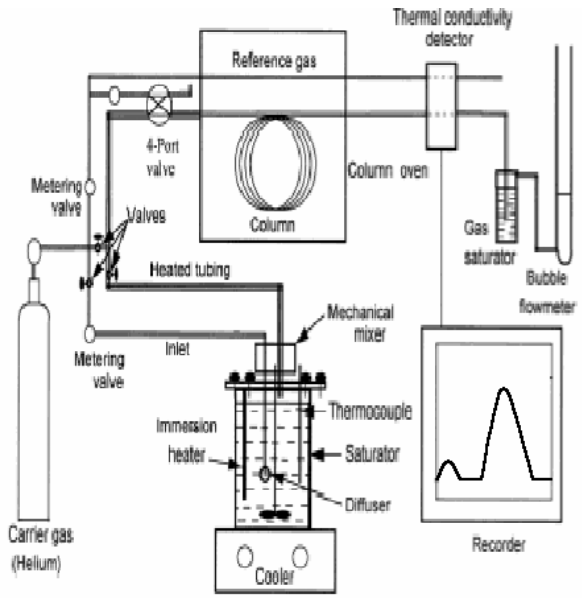

Figure 5.1. Experimental Set-up of IGC System

IGC has been used primarily for the measurement of solution thermodynamic parameters (Pawlish et al., 1987). When an IGC experiment is carried out at temperatures significantly higher than the glass transition temperature of the polymeric stationary phase, the retention time is determined by the solubility of that component in the polymer. Consequently measurements of retention time can be used to calculate such useful parameters as Henry's law constant, the activity coefficient, and also diffusion of the solute in the polymer phase. The speed and cost are the advantages of this method.

5.2. Piezoelectric Crystal

Quartz crystal resonators are simple tools for determining the weight of thin films. When a thin film is cast onto one of the electrodes of a thickness shear resonator, its acoustical resonance frequencies change due to weight of the film changing during the sorption. The relation between the amount of vapour sorbed and the frequency decrease is linear at low mass loading. Thus, the step change of solvent temperature sent to the system is kept very small. In essence, the piezoelectric crystal acts as a very sensitive microbalance. With reasonable assumptions for the stability of the crystal's base frequency and the precision of the frequency counter employed, the piezoelectric method allows the detection of as little as 10 nanograms of solvent using a 10MHz crystal (Saby-Dubreuil, 2001).

Figure 5.2 illustrates the experimental set-up of piezoelectric crystal sorption system. The frequency of bare, uncoated crystal is measured under vacuum. Then polymer film is deposited by casting a known volume of polymer solution onto the crystal on a known area. After film is partially dried, the crystal is placed in the chamber and thoroughly dried and the frequency of coated crystal is measured under vacuum. Finally, penetrant at constant temperature is introduced to the chamber and the frequency is recorded as a function of time. In this experimental technique, the use of ultra clean, temperature controlled vacuum chamber is critical.

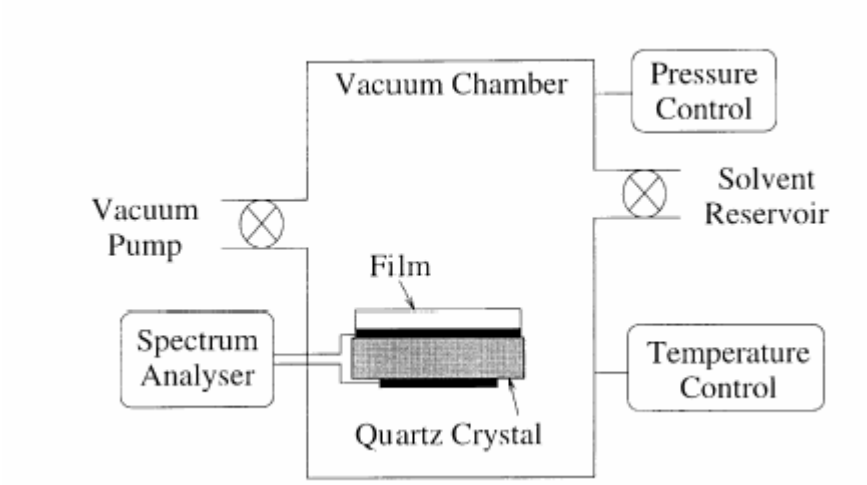

Figure 5.2. Experimental set-up of piezoelectric crystal sorption system (Saby-Dubreuil et.al, 2001)

5.3. Gravimetric Sorption Techniques

5.3.1. Cahn Electro Balance

Cahn vacuum electro balance immersed in a constant air bath allows to monitor the sorption process as shown in Figure 5.3. The apparatus consists of three main coupled components: a Cahn electrobalance weighing unit, a solvent supply system and a computer. Solvent vapor is produced by a boiler where vapor pressure in the boiler is

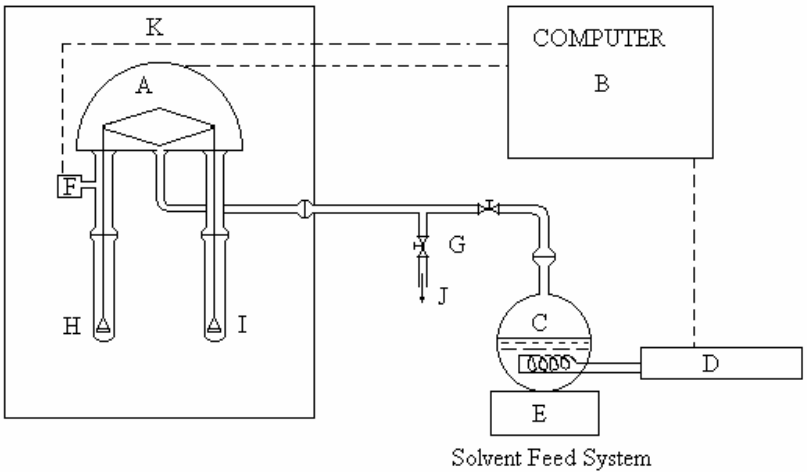

Figure 5.3. Oscillatory sorption apparatus (Vrentas et.al.1984). A- electrobalance, B- minicomputer and associated components, C- solvent boiler, D- power supply, E- cooler and magnetic stirrer, F- pressure transducer, G- vacuum valves, H- polymer sample, I- tare weight, J- vacuum pump, K- constant temperature air bath.

controlled by the temperature of the liquid. The solvent vapor pressure in the sorption chamber is measured with a pressure transducer and the analog signal is programmed so that the desired vapor pressure relationship is calculated as a function of time. Experiments with the Cahn Electrobalance are limited to temperatures below 55°C. In addition, the balance is affected by the organic solvent vapor.

5.3.2. Quartz Spring Balance

A widely used device for gravimetric sorption is the McBain spring balance. A thin, uniform polymer film is placed at the end of a calibrated spring and contacted with penetrant at fixed pressure. As penetrant sorbs into the polymer matrix, the load on the spring increases, and the spring extends. The time dependent mass uptake of penetrant by the polymer is measured by recording the spring extension. Typically such measurements are made using a manual

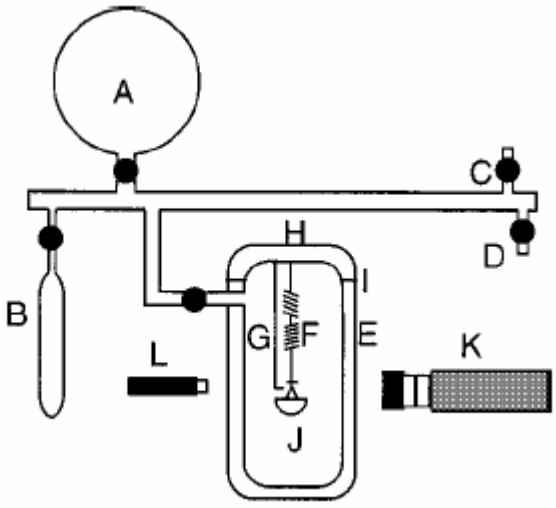

Figure 5.4 Experimental set-up of quartz spring balance sorption system (McDowell C.C., et.al. (1998)

cathetometer to observe the position of the spring relative to a reference rod of fixed length. Figure 5.4 presents a schematic of the sorption system. A glass bulb, A, which is part of a glass manifold is used as a penetrant vapor reservoir. Liquid penetrant is stored

in a glass ampule, B, before being vaporized into the glass manifold. Alternately, gaseous penetrant can be introduced into the system by connecting a gas cylinder to the manifold in place of the ampule. A ventilation valve, C, is used to expose the system to air at ambient conditions. The system is connected, via valve D, to a vacuum pump used for sample degassing and system evacuation. The water-jacketed vessel, E, provides temperature control for the sample environment. The glass manifold is wrapped with heating tape, which is connected to variable autotransformers for temperature control. Alternatively, the system can be placed in a temperature-controlled box. A sensitive quartz spring, F, and reference rod, G, are suspended from the cap of the vessel, H, which is sealed to the main vessel with an O-ring seal, I, and a metal clamp. The polymer sample is hung directly on a hook at the end of the spring.

5.3.3. Magnetic Suspension Balance

Magnetic suspension balance (MSB) developed by Kleinrahm and Wagner (1986) is one of the most reliable and sensitive apparatus among other gravimetric sorption equipment such as quartz spring balance, or microbalance.

The MSB has many advantages similar to microbalances except that the sample and the balance are separated from each other. As a result, the microbalance can not be damaged or disturbed from the measuring atmosphere. This type of instrument is expected to be suitable for the measurement of solubility and diffusivity of polymer-solvent system at high temperatures and high pressures. The MSB allows for sorption measurements with a pure gas in the pressure range from high vacuum to 150 bar at temperatures up to 473 K. High-resolution (1μg) and high accuracy (0,002%) can be achieved. Magnetic suspension coupling separates the microbalance from the measuring atmosphere. This coupling shown in Figure 5.5 consists of an electromagnet, which is attached at the underfloor weighing hook of the balance outside the measuring cell, and a suspension magnet which is inside the measuring cell to which the sample sorbent is connected.

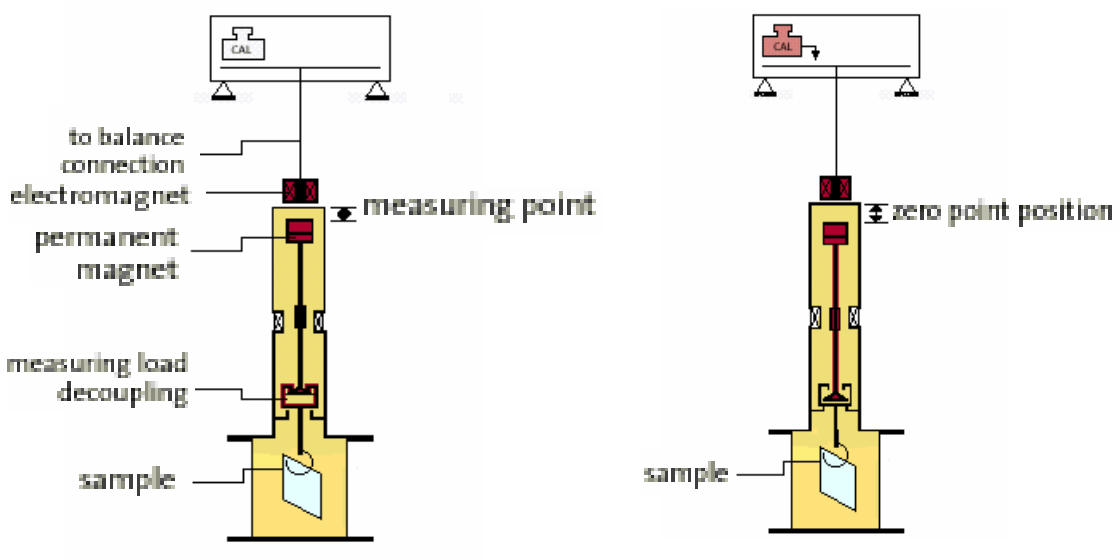

Figure 5.5. Magnetic suspension Balance

By using the magnetic suspension coupling the measuring force is transmitted contactlessly from the measuring chamber to the microbalance while the suspension magnet and the sample sorbent achieve a constant vertical position by modulating the electromagnet voltage by a controlling unit. The suspension magnet, which is used for transmitting the force, consists of a permanent magnet, a sensor core, and a device for decoupling the measuring load. The measuring load decoupling allows to set down the sample on a support by varying the vertical position of the permanent magnet, which is realized by the controlling unit. When the sample set down, the sample and permanent are decoupled, only the permanent magnet is in suspension and only its mass is transmitted to the microbalance. This zero point position allows a taring and calibrating of the balance at all times, even while recording measurements. This can enhance the accuracy of the measurements considerably because long sorption times are generally needed.

Thermostated jacket allows constant temperature in the measuring cell and the shape of the measuring cell is well designed because there is no temperature deviation between one point to another point in the measuring cell.

CHAPTER 6

LITERATURE SURVEY

In this study mutual diffusion coefficient of methylmethacrylate monomer in acrylic copolymer composed of MMA and BA was measured by using a new type of gravimetric sorption apparatus called magnetic suspension balance. Although this acrylic copolymer is consumed in large amounts in paint industry, there are no diffusivity data in the literature for this copolymer. Many investigators studied diffusion behavior of monomers or solvents in pure acrylic homopolymers such as polymethylmethacrylate, or polybutylmethacrlate.

6.1. Diffusivity Studies in Acrylic Polymers

Faldi, A., et al., (1994) have measured self diffusion coefficient of methylmethacrylate (MMA) in poly(methylmethacrylate) (PMMA) at 50°C. The concentration range of measurements were 0 to 100% by weight of MMA. Diffusion coefficient was obtained as $2.5x10^{-5}cm^2/s$ when the MMA concentration in PMMA was close to one, when the concentration of MMA in PMMA was 0.1 the diffusion coefficient decreased approximately 8 orders of magnitude. A correlation was developed in order to calculate the variation of glass transition temperature (T_g) of polymer against the monomer concentration. At above and below the glass transition temperature of the polymer the diffusion coefficients indicated large variation as given in Table 6.1. Authors obtained that when the MMA concentration was 0.15, the glass transition temperature of the polymer was below 50°C.

Table 6.1. Self diffusion coefficients of MMA in PMMA at 50°C

Weight fraction of MMA (ω_1)	$D_{MMA-PMMA}$ (cm^2/s)
1	$2.5x10^{-5}$
0.595	$6.0x10^{-6}$
0.3	$4.x10^{-7}$
0.21	$5.2x10^{-9}$
0.15	$7.1x10^{-10}$
0.1	$1.97x10^{-13}$

Tonge-Gilbert (2001) measured self diffusion coefficient of MMA and butylmethacrylate (BMA) monomers in polybutylmethacrylate (PBMA) and PMMA matrices using Pulsed Field Gradient Nuclear Magnetic Resonance (PFGNMR) technique. Experimental data were compared with the predictions from free volume theory as shown in Figure 6.1 through 6.4. The agreement between the predicted and experimental diffusion coefficient was found to be good for MMA in PMMA, moderate for MMA in PBMA, and very poor for BMA in PBMA. Authors claimed that the discrepancy between experimental and predicted diffusion coefficient is due to lack of energy contribution (activation energy=0) in the free volume theory. As a result Tonge and Gilbert (2001) suggested that using activation energy in the prediction of diffusivities might improve the agreement between the theoretical and experimental

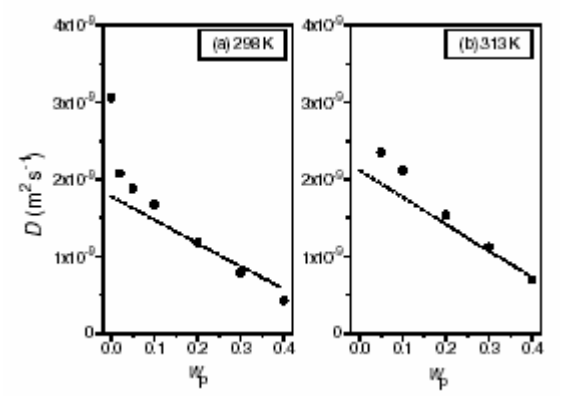

Figure 6.1. Predicted (dashed line, as obtained with the completely a priori treatment) and the observed diffusion coefficient for MMA in PMMA: (a) at 298 K; (b) at 313 K

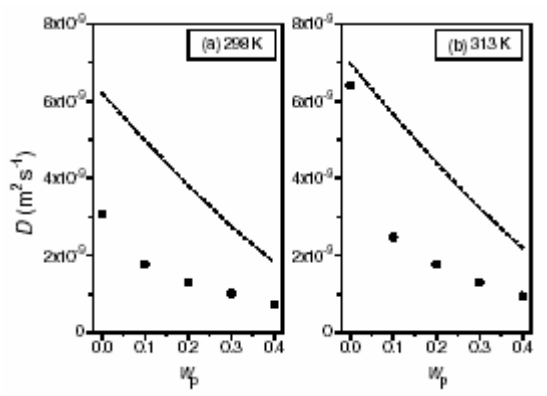

Figure 6.2. Predicted (dashed line, as obtained with the completely a priori treatment) and the observed diffusion coefficient for MMA in PBMA: (a) at 298 K; (b) at 313 K

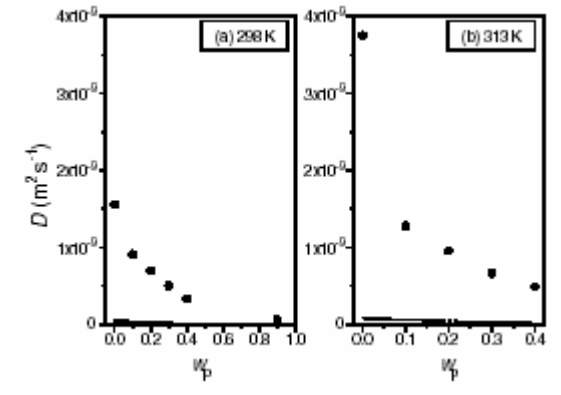

Figure 6.3. Predicted (dashed line, as obtained with the completely a priori treatment) and the observed diffusion coefficient for BMA in PBMA: (a) at 298 K; (b) at 313 K

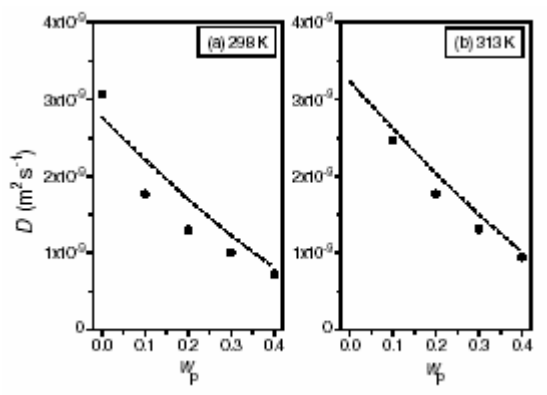

Figure 6.4. Predicted (dashed lines) and observed diffusion coefficients (individual points) for MMA in PBMA, using E^*=2 kJ/mol: (a) at 298 K; (b) at 313 K

Kobuchi and Arai (2002) have measured the mutual diffusion coefficients for acrylic adhesive+acetate ester, acrylic adhesive+ketone and poly-2-ethylhexylmethacrylate +ketone systems using quartz spring. They reviewed the prediction performances of the free volume theory for those systems. They have proposed a new method for estimating the parameters in Equation 2.1 from the physical properties of the solvent.

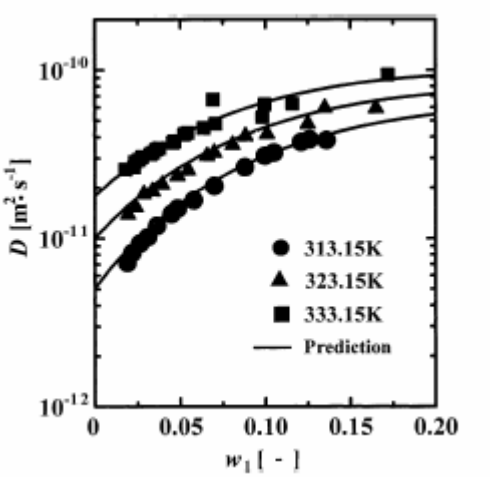

Figure 6.5. Comparison between the experimental and predicted mutual diffusion coefficients for acrylic adhesive + propyl acetate system.

These parameters $\left(D_0, E, \xi, \chi, M_1\hat{V}_1^*, \gamma_1\right)$ were correlated with the molecular weight, the cohesive energy and the molar volume at the normal boiling point. The mutual diffusion coefficients calculated for acrylic adhesive + propyl acetate system is shown in Figure 6.5. The symbols and solid lines in this figure represent the experimental and predicted values, respectively. As shown in Figure 6.5, the predicted results are in good agreement with the experimental data.

6.2. Diffusion Studies Conducted with Magnetic Suspension Balance

Magnetic suspension balance was used by a Japanese group (Sato et al., 2001) to measure solubility of carbon dioxide (CO_2) in polyvinylacetate (PVAC) at temperatures from 313 to 373K and pressures up to 20 MPa. They have shown that magnetic suspension balance can be used accurately for high temperature and high-pressure solubility and diffusivity measurements. Author have mentioned about the

characteristics of the magnetic suspension balance, and also compared other conventional sorption equipment.

Mamaliga et al., (2003) have measured solubility and diffusion coefficients of methanol and toluene in Poly(vinylacetate) by means of magnetic suspension balance at 20, 40 and 60°C. Experimental solubility data were correlated with the Flory-Huggins and UNIFAC-free volume model and were compared with the previous results from the literature. The solubility measurements of methanol and toluene in PVAc system agree with the literature data except at higher activities. The experimental diffusion coefficients were correlated with Vrentas and Duda free volume theory with and without thermodynamic factor. Predicting self diffusion coefficients of toluene-PVAc system at 20 and 60°C by using parameters obtained at 40°C, indicated higher accuracy over a wide concentration range.

CHAPTER 7

EXPERIMENTAL

7.1. Materials

In this study the acrylic copolymer consisting of methylmethacrylate (MMA) and butylacrylate (BA) and the MMA monomer (CAS number 80-62-6) were supplied by Organik Kimya A.Ş. Turkey. The polymer sample was received in the form of an emulsion consisting of 50% copolymer and 50% water by volume. The copolymer contains 110 ppm residual methylmethacrylate.

7.2. Film Preparation Method

Preparation of a polymer film influences the structure of the film formed, which plays an important role on the diffusion behavior. Polymer films with different thicknesses were prepared by casting the solution on a clean and smooth glass substrate through an automatic film applicator-1133N. The cast film was put into an oven maintained at a temperature of 40°C under vacuum for 30 minutes. To remove the film from the glass substrate, the sample was held in the water bath at a temperature of 40°C. Then, the film was put into the vacuum oven adjusted at a temperature of 125°C and kept in the oven for one day. Finally, to remove all the residual methylmethacrylate and water in the sample, the temperature of the oven was raised to 140°C and the sample was kept inside the oven for 3 days. The thickness of the sample was measured from 20 different points and average thickness of the sample was calculated based on these measurements.

7.3. Characterization Studies

7.3.1. Differential Scanning Calorimetry (DSC) Analysis

Differential Scanning Calorimetry (DSC) was used to observe various thermal events, which are the glass transition, crystallization, and melting. To perform the

analysis (Shimadzu DSC 50), 9 mg polymer sample was placed in an aluminium pan and heated at a constant rate from 20°C until 500°C under an inert atmosphere. The flow rate of nitrogen gas was kept at 40ml/min and the rate of increase in temperature was 1°C/min until 30°C and it was increased to 5°C/min above 30°C.

7.3.2. Thermal Gravimetric Analysis (TGA)

Thermal gravimetric analysis (TGA) was performed to determine the degradation temperature of the copolymer. For this purpose, 9.46 mg sample was placed in an aluminum pan and heated continuously from 20°C to 600°C at a rate of 10°C/min. Analysis was performed with Shimadzu TGA51 under nitrogen flow at a rate of 30ml/min.

7.3.3. Fourier Transform Infrared Spectroscopy (FTIR) Analysis

Fourier Transform Infrared Spectrophotometer (Shimadzu 8601) was used between the wavenumber of 400 and 4000 cm^{-1} to obtain the functional groups in the acrylic copolymer sample. Polymer films described in the section of film preparation method (7.2) were used in FTIR analysis.

7.3.4. Nuclear Magnetic Resonance (NMR) Analysis

To determine the composition of the acrylic copolymer film composed of methyl methacrylate and n-butyl-acrylate monomers ^{1}H NMR spectrum was taken at Iowa State University, in Chemistry Department.. A spectrum was obtained at 302 K in a deuteriochloroform ($CDCl_3$) solution using a Varian type spectrometer operating at 400MHz. The parameters for the proton spectra were as follows: spectral width: 6000 Hz, acquisition time: 3.729sec.

7.3.5. Scanning Electron Microscope (SEM) Analysis

For scanning electron microscope (Philips, XL-30SFG) analysis two small pieces of polymer films were cut by scissors and one of them was used to investigate

the film morphology and the other was used for measuring average thickness of the films.

7.4. Measurements of Dynamic and Mechanical Properties of Copolymer Sample

The rheological measurement of the copolymer sample was performed by a rheometer (Rheometrics Mechanical Spectrometer/Dynamic Spectrometer (RMS-800/RDS-II), Serial No: 035-024) at Illinois Institute of Technology, in Department of Chemical Engineering.

25mm parallel plates were used as the geometry for the experiment. Circular disc shaped samples was punched out of 22.5mm diameter and was stacked over each other to form 1mm thick sample. Then the sample was loaded on to the fixtures and squeezed to a gap of 0.64mm making the sample diameter 25mm (at one specific temperature). This technique was used for all the temperatures (50°C, 75°C, 100°C, 125°C and 150°C). After equilibration, strain controlled small amplitude frequency sweep experiment was done in order to measure loss modulus, G', and storage modulus, G'', of the copolymer sample.

The master curve and the shift factors were found by performing time-temperature superposition at a reference temperature of 100C.

7.5. Experimental Set-up and Procedure

The experimental set-up shown in Figure 7.1 consists of three main parts. The main sorption column, control unit, and supporting units (constant temperature baths, cold trap, heating tape, temperature controller, vacuum pump, pressure gauge and also ball valves).

The main sorption chamber (measuring cell) is enclosed by the high-pressure flange. The polymer sample is put into a bucket and the bucket is suspended from a permanent magnet. The resolution of the balance is 1μg, the maximum load is 5 g, and the reproducibility of the measurements is ±2μg. The cell can withstand to high pressures up to 150 bars and temperature up to 250°C in the coupling housing. The upper part of the column is made of copper chrome zirconium, the inner surface is gold

plated. The lower part is made of stainless steel. The steel between these two parts is metal seal coated with gold. All other inner parts are made of stainless steel. Double tube thermostat around the column allows circulating fluid and maintaining constant temperature in the column. Pt100 temperature probe inserted into the column just below the sample holder measures the temperature of the fluid in the column.

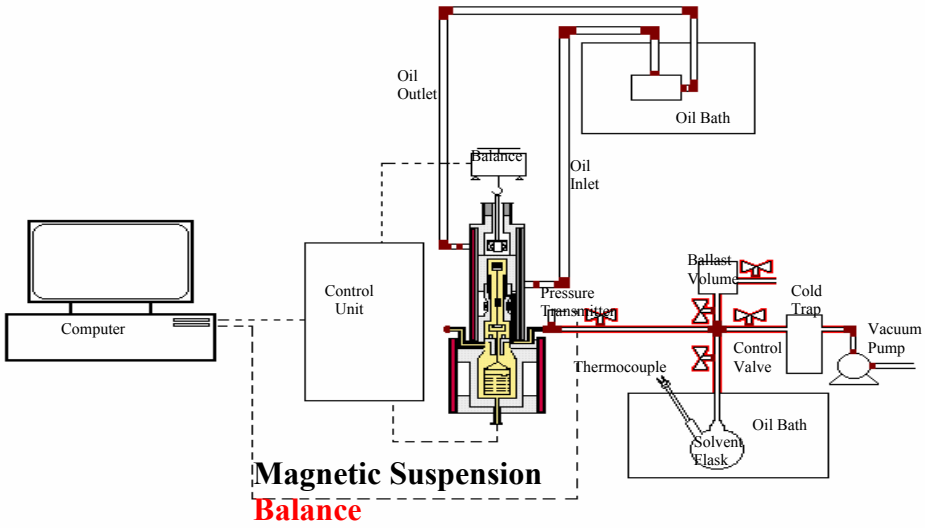

Figure 7.1. Experimental Set-up

Operation of the balance is automatically controlled by software, which also collects the measurements of mass changes and temperature. Solvent vapor is prepared in a solvent flask inserted into a constant temperature bath which works between room temperature and boiling point of the solvent (accuracy ±0.5°C). The vapor pressure of the solvent is measured by a pressure transducer operating within a range of vacuum up to 1 atm. with an accuracy of 0.25% full scale. Heating tape is used on all solvent vapor line to prevent condensation of solvent vapor. The heating rate of the tape is controlled by using a temperature controller (Love controller) which enables to give accuracy of 0.25% full scale.

All tubings are made of stainless steel and all valves exposed to solvent vapor are made of teflon. To prevent damage to the vacuum pump, a cold trap made of pyrex is placed between the column and the pump.

At the beginning of a typical experiment, sample is placed into the column and evacuated with a vacuum pump, which can provide vacuum levels up to 10^{-4} mbar. The

column is evacuated for at least 24 hours to maintain constant reading as well as to evacuate the column completely. When vapor-liquid equilibrium is achieved in the solvent flask at the desired temperature of the solvent, then solvent vapor is sent into the column by opening the valve. The weight change of the sample is followed as a function of time. Once the polymer sample reaches an equilibrium state at a specific penetrant vapor pressure level, the valve is closed and an abrupt increase in the vapor pressure of the solvent is induced by increasing the temperature of the constant temperature bath. The step change in the column is produced by opening the valve and letting solvent vapor at a new vapor pressure level into the column. The number of runs in a given series for each temperature depends of the amount of the penetrant absorbed. Usually step size is adjusted to make the difference between the equilibrium and initial mass of the penetrant small. This adjustment allows assuming constant diffusivity within this range and negligible swelling of the polymer film. Consequently, the analytical solution given in Equation 3.6 can be used to determine the diffusivity from the experimental measurements.

7.5.1. Forces Affecting the System

Since the weight of polymer film which is used in the sorption experiments is in the range of 5-15 milligrams then the amount of absorbed solvent is in the level of micrograms. Buoyancy of solvent vapour in the measuring cell affects the measurement and thus the buoyancy of the substrate at different vapour pressures and hence different densities should be taken into account. Whole forces affecting the system were marked in Figure 7.2. A balance of forces for the whole system gives an equation for the determination of the amount of solvent vapour absorbed by the polymer sample. The absorbed amount of vapour can be determined by a balance of forces in vertical direction.

These forces are:

$AF_1 = m_{absorbed} \bullet g$, the force resulting from the absorption of an amount of vapor by the sample,

$GF = m_{vac} \cdot g$, gravitational force affecting the system in the vacuum,

$MF = S_{MP} \cdot g$, measurement force or signal detected by the balance

$AF_2 = \rho_{vapour} \cdot \lfloor V_{cage+hook} + V_{sample+vapour} + V_{samplecage} \rfloor \cdot g$, ascending force affecting the system

Balance of forces gives:

$$AF_1 + GF = MF + AF_2$$

Then, amount of absorbed vapor can be obtained as follows:

$$m_{absorp} = S_{MP} + \rho_{vapour} \cdot \lfloor V_{cage+hook} + V_{sample+vapour} + V_{samplecage} \rfloor - m_{vac} \quad (7.1)$$

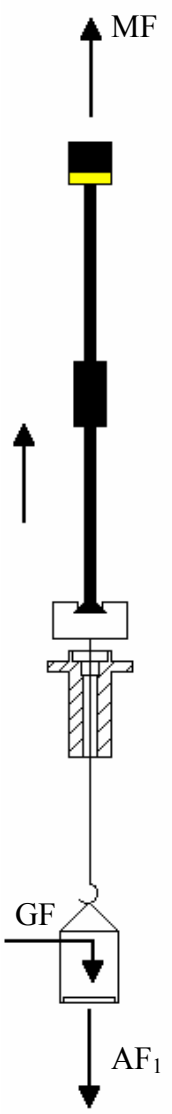

Figure 7.2. Forces affecting the system

CHAPTER 8
RESULTS AND DISCUSSIONS

8.1. Characterization of the Polymer Films

8.1.1. Determination of the Morphology and the Thickness of the Films

Figure 8.1 shows the SEM picture of cross section of the copolymer film. Nonporous, homogenous film structure was observed indicating that diffusion path is through the overall thickness of the film. Figure 8.2 illustrates how SEM picture was utilized to measure film thickness from different positions.

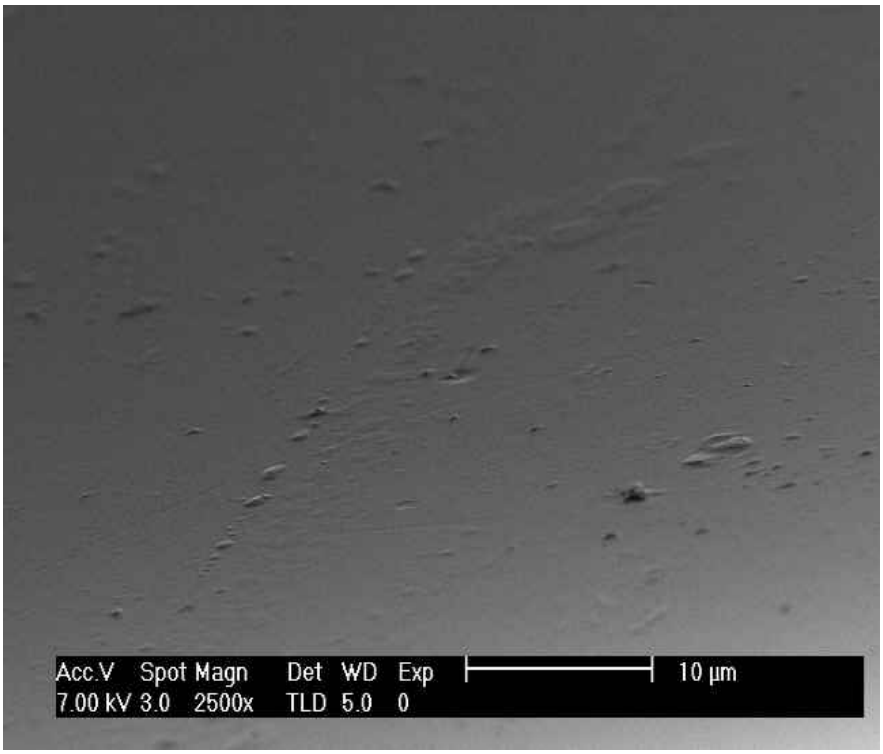

Figure 8.1. SEM picture of the surface of MMA-BA copolymer

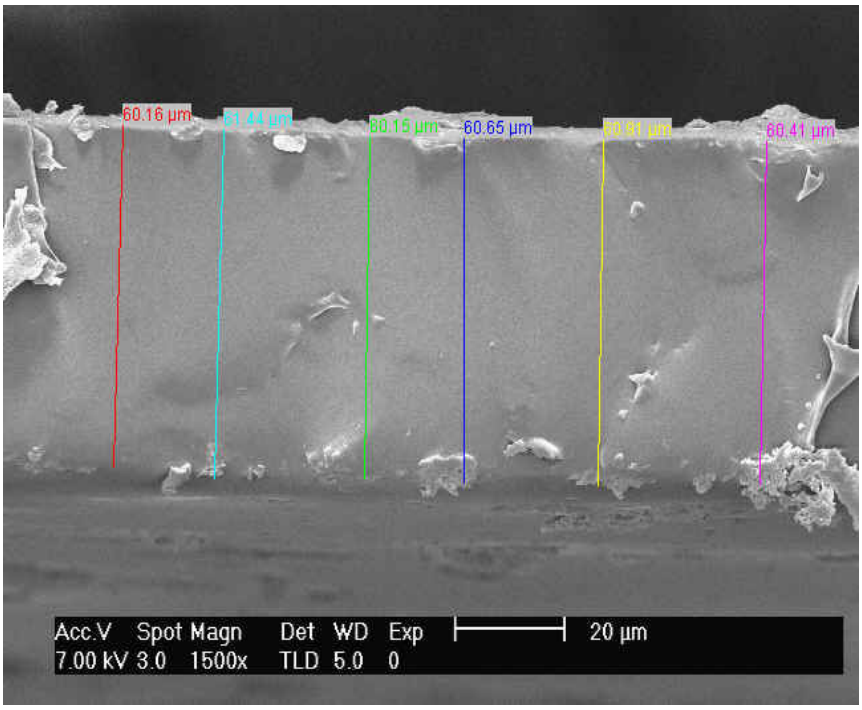

Figure 8.2. SEM picture showing the cross section of MMA-BA copolymer film used to measure film thickness.

8.1.2. Differential Scanning Calorimetry (DSC) Analysis

Figure 8.3 shows the DSC curve of the MMA-BA copolymer. In DSC, energy is supplied to both sample and a reference material and the difference between the sample and the reference is used as a measure of thermal events mentioned above. As seen from Figure 8.3, at low temperatures the change in the amount of energy given to the sample is small compared to the reference, thus, heat flow curve remains constant. Between 35°C and 41°C, a sharp decrease in the slope of the heat flow curve is observed which corresponds to glass transition. From this decrease, the glass transition temperature of the copolymer was determined as 40.9°C. Between 41°C and 300°C, heat flow curve again remains constant which indicates that no change in the structure of the polymer takes place. Amount of heat given to the sample compared to the reference increases significantly above 300°C and a negative peak was observed due to degradation of the polymer. The heat of degradation was determined as –73.01 cal/g from the area under the line drawn between 343°C and 418°C.

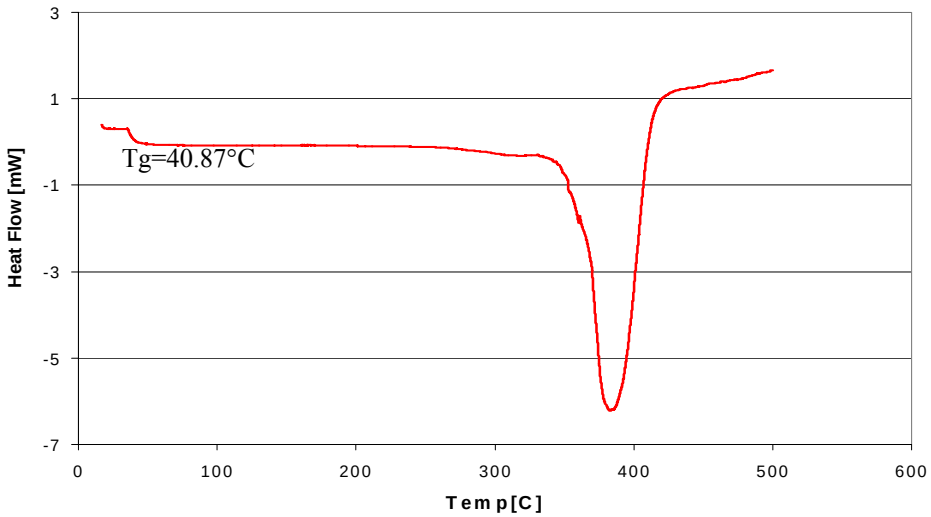

Figure 8.3. Differential Scanning Calorimetry analysis of MMA-BA copolymer

8.1.3. Thermal Gravimetric Analysis (TGA)

Figure 8.4 shows TGA curve of the MMA-BA copolymer. According to this figure, weight loss of the sample is observed above 100°C. The weight loss up to 300°C is attributed to the loss of water remained in the film. Significant weight loss due to degradation of the polymer starts at 300°C and when temperature is above 500°C, almost all of the polymer degrades.

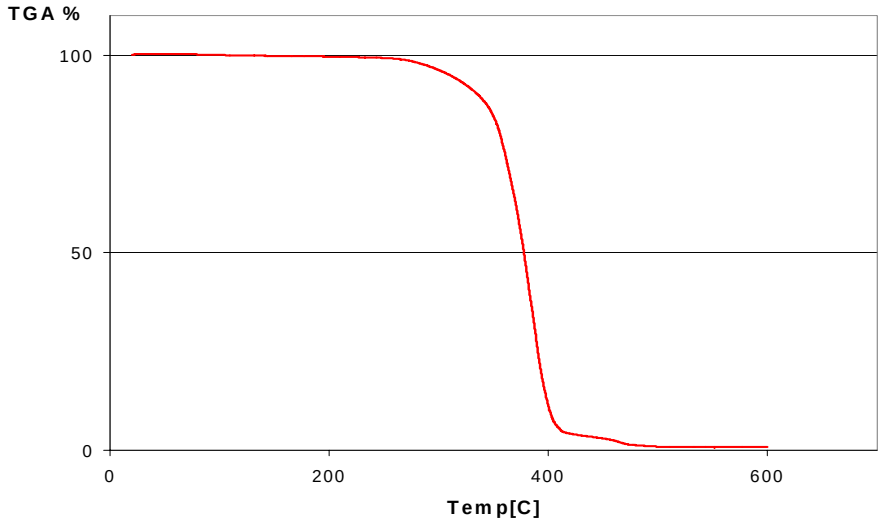

Figure 8.4. Thermal Gravimetric Analysis of MMA-BA copolymer

8.1.4. Fourier Transform Infrared Spectroscopy (FTIR) Analysis

FTIR analysis shown in Figure 8.5 gives expected functional groups in the copolymer sample. The spectrum shows a sharp intense peak at 1731 cm^{-1}, which can be attributed to the presence of C=O stretching vibrations. The broad peak ranging from 1260 to 1000 cm is due to C–O (ester bond) stretching vibrations. The broad band from 950 to 650 cm is due to C–H bending. The sharp peak from 3000 to 2900 cm is due to the presence of C–H stretching vibrations

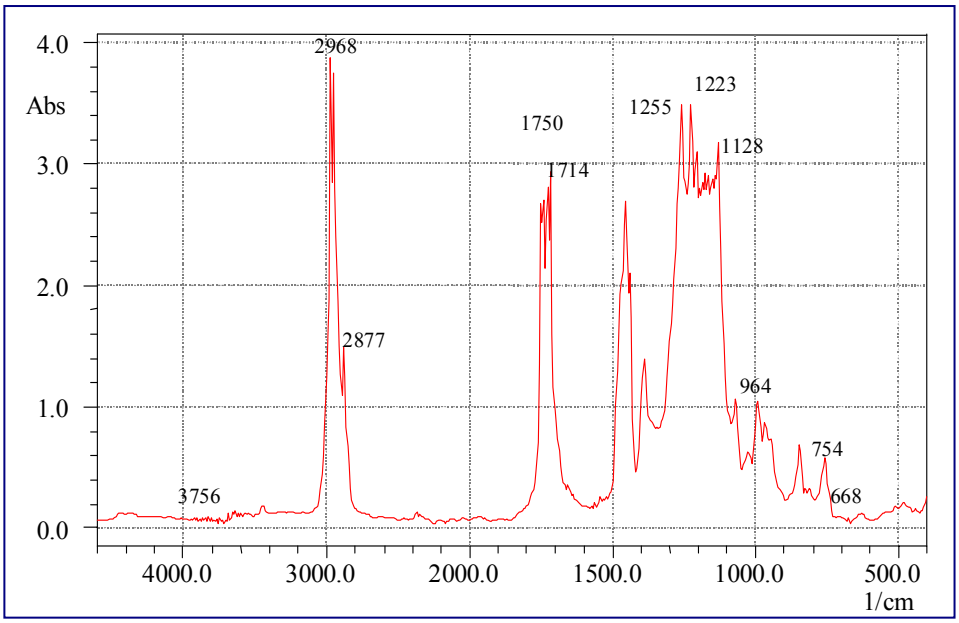

Figure 8.5. Fourier Transform Infrared Spectroscopic Analysis of MMA-BA copolymer

8.1.5. Nuclear Magnetic Resonance (NMR) Analysis

Figure 8.6 shows NMR spectrum of MMA-BA copolymer. The rather complicated collection of NMR lines occurring between 0.5-2.5 ppm are assigned to the alkyl methylene and methyl protons of the copolymer. The two isolated NMR lines occurring at ≈3.6 and 3.9 ppm are assigned to the three protons of the $–OCH_3$ methoxy substituent of MMA and the two alkoxy protons of the $–OCH_2$ methylene group respectively. Thus, if the relative areas of these two NMR lines are divided by 3 and 2

respectively as given in Equation 8.1, quantitative compositional analysis becomes remarkably straightforward.

$$\%MMA = \frac{A_{3.6\,ppm}/3}{A_{3.6\,ppm}/3 + A_{3.9\,ppm}/3} x100 \qquad (8.1)$$

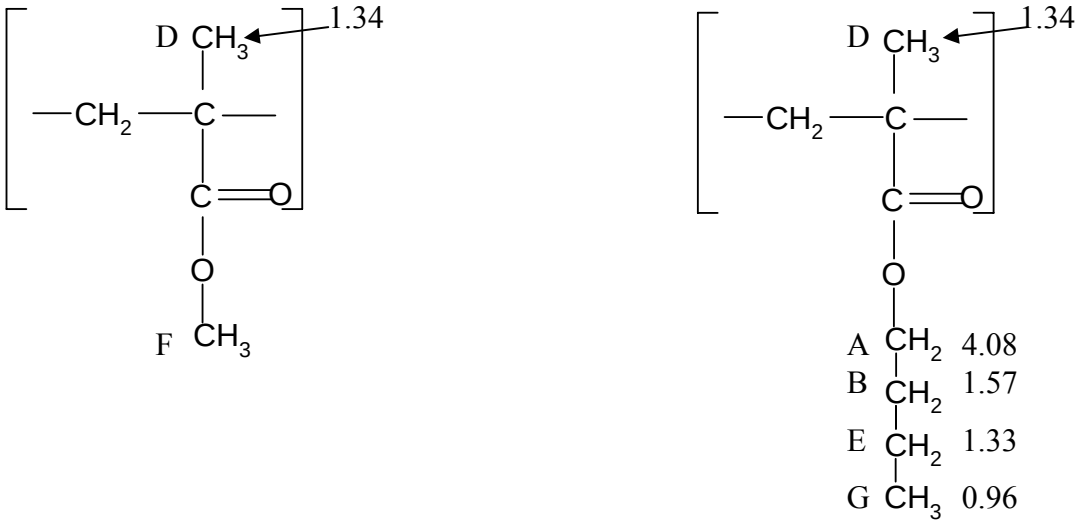

By using corresponding areas determined from the spectrum shown in Figure 8.6, the compositions of MMA and BA in the copolymer were calculated as %19.7 wt. % and %80.3 wt. %, respectively.

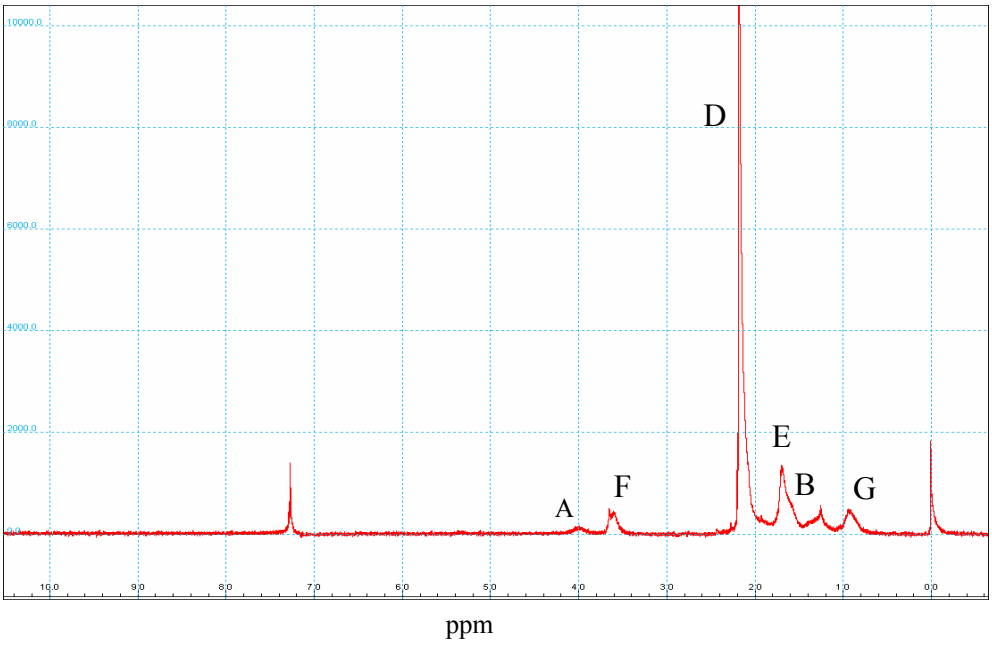

Figure 8.6. ^{1}H NMR spectra of MMA-BA copolymer

8.2. Determination of Free Volume Parameters of MMA and MMA-BA Copolymer System

8.2.1. Determination of Free Volume Parameters of MMA

The free volume parameters of MMA were obtained from Equation 2.9 using viscosity data given in Table 8.1. Three unknown parameters in Equation 2.9 were obtained as follows by minimizing the difference between the experimental and theoretical viscosity values. $A_1 = 0.086538cp$, $\frac{\gamma \hat{V}_1^*}{K_{11}} = 332.63K$, $K_{21} - T_{g1} = -120.2K$

Table 8.1. Viscosity temperature data of MMA [Riddle, 1954]

η(cp)	T (K)
0.76	273.15
0.63	288.15
0.56	298.15
0.45	323.15
0.38	343.15

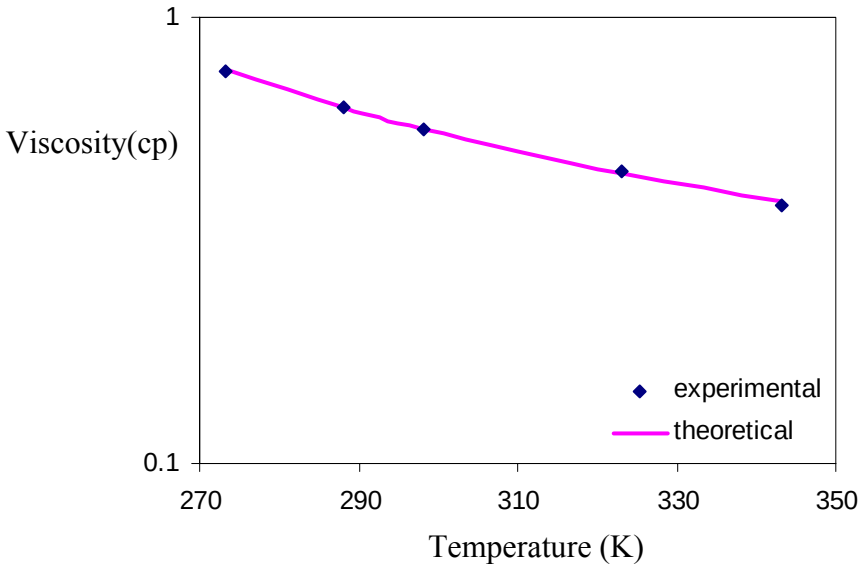

Figure 8.7. Comparison of the experimental and the theoretical viscosities obtained from Equation 2.9.

Figure 8.7 illustrates the comparison of the experimental and the theoretical viscosity values with respect to temperature. The agreement between the experimental and theoretical values is perfect indicating that the free volume parameters obtained from Equations 2.10 and 2.11 are correct.

8.2.2. Determination of Free Volume Parameters of the MMA-BA Copolymer

Specific hole free volume of MMA-BA copolymer, $\hat{V}_2^*$, was calculated by using the specific hole free volumes of Polymethylmethacrylate (PMMA) and Polybutylacrylate (PBA) and the composition of MMA-BA copolymer obtained from NMR analysis.

$$\hat{V}_{2copolymer}^* = x_{MMA}\hat{V}_2^*\big|_{PMMA} + x_{BA}\hat{V}_2^*\big|_{PBA} \qquad (8.2.)$$

The weight fraction of MMA and BA were converted into mole fraction $x_{MMA} = 0.24$ and $x_{BA} = 0.76$. By taking the specific hole free volume of MMA and BA as 0.789 and 0.843 cm^3/g respectively, $\hat{V}_2^*$ of copolymer was calculated as $0.83 cm^3/g$.

The free volume parameters of the copolymer, K_{12}/γ and $K_{22} - T_{g2}$ were obtained by first determining WLF constants from Equation 2.12. The proper relationship between the shift factor, a_T, and temperature was obtained by measuring loss modulus, G', and storage modulus, G'' of MMA-BA copolymer as a function of frequency. The loss modulus and the storage modulus values measured at 50°C, 75°C, 100°C, 125°C and 150°C were reported in Table 8.2. Figure 8.8 shows master curve of MMA-BA copolymer obtained by shifting the data in Table 8.2 until they over lap. The shift factor, a_T, as a function of temperature is given in Figure 8.9.

By minimizing the difference between the experimental and theoretical shift factor from Equation 2.12, with a reference temperature of T_{ref}=100°C, WLF parameters were determined as follows:

C_1=11.94 C_2=231.8,

Then, from Equations 2.10 and 2.11, the free volume parameters of the copolymer were calculated as follows:

K_{12}/γ =1.302x10^{-4}cm^3/g.K, $K_{22} - T_{g2}$ =-81.2K

Table 8.2. Loss modulus, G', and the storage modulus, G'', of MMA-BA copolymer as a function of frequency measured at 50 °C, 75 °C, 100 °C, 125 °C ve 150 °C.

50 °C			75 °C			100 °C			125 °C			150 °C		
$\omega x10^{2}$	$G'x10^{-6}$	$G''x10^{-6}$	$\omega x10^{2}$	$G'x10^{-5}$	$G''x10^{-5}$	$\omega x10^{2}$	$G'x10^{-5}$	$G''x10^{-4}$	$\omega x10^{2}$	$G'x10^{-5}$	$G''x10^{-4}$	$\omega x10^{2}$	$G'x10^{-5}$	$G''x10^{-4}$
1	1.4	$4.85x10^{5}$	1.00	5.09	1.82	1.00	2.36	6.92	1.00	1.70	3.52	1.00	1.57	2.29
1.58	1.53	$5.38x10^{5}$	1.58	5.61	2.05	1.58	2.59	7.93	1.58	1.82	4.04	1.58	1.68	2.57
2.51	1.67	$6.04x10^{5}$	2.51	6.22	2.25	2.51	2.82	8.99	2.51	1.95	4.58	2.51	1.77	2.91
3.98	1.83	$6.90x10^{5}$	3.98	6.90	2.49	3.98	3.10	10.2	3.98	2.09	5.22	3.98	1.86	3.31
6.31	2.00	$8.03x10^{5}$	6.31	7.63	2.71	6.31	3.40	11.4	6.31	2.25	5.91	6.31	1.96	3.77
10	2.21	$9.57x10^{5}$	10.0	8.44	2.98	10.0	3.74	12.9	10.0	2.42	6.72	10.0	2.08	4.30
15.8	2.43	$1.16x10^{6}$	15.8	9.36	3.26	15.8	4.13	14.5	15.8	2.62	7.64	15.8	2.20	4.90
25.1	2.70	$1.44x10^{6}$	25.1	10.3	3.55	25.1	4.56	16.2	25.1	2.84	8.66	25.1	2.35	5.57
39.8	3.03	$1.82x10^{6}$	39.8	11.4	3.86	39.8	5.05	18.1	39.8	3.10	9.81	39.8	2.51	6.37
63.1	3.44	$2.34x10^{6}$	63.1	12.5	4.21	63.1	5.59	20.2	63.1	3.38	11.1	63.1	2.69	7.25
100	3.94	$3.04x10^{6}$	100	13.7	4.62	100	6.20	22.3	100	3.71	12.6	100	2.90	8.29
159	4.58	$4.00x10^{6}$	159	15.0	5.11	159	6.87	24.6	159	4.09	14.2	159	3.15	9.45
251	5.39	$5.32x10^{6}$	251	16.4	5.74	251	7.60	26.9	251	4.51	16.0	251	3.42	10.8
398	6.43	$7.14x10^{6}$	398	17.9	6.53	3.98	8.41	29.4	3.98	4.99	17.9	3.98	3.74	12.2
631	7.79	$9.66x10^{6}$	631	19.6	7.59	6.31	9.28	32.2	6.31	5.53	20.0	6.31	4.10	13.9
1000	9.57	$1.32x10^{7}$	1000	21.5	9.03	1000	10.2	35.2	1000	6.12	22.2	1000	4.52	15.8
1590	11.9	$1.80x10^{7}$	1590	23.6	11.0	1590	11.2	38.5	1590	6.79	24.6	1590	4.98	17.8
2510	15.0	$2.47x10^{7}$	2510	26.2	13.6	2510	12.3	42.5	2510	7.51	27.2	2510	5.51	20.0
3980	19.1	$3.38x10^{7}$	3980	29.3	17.0	3980	13.5	47.5	3980	8.30	29.9	3980	6.10	22.5
6310	18.7	$3.28x10^{7}$	6310	33.1	21.8	6310	14.7	53.9	6310	9.17	33.0	6310	6.75	25.1
10000	13.1	$1.37x10^{7}$	10000	37.7	28.0	10000	16.0	62.2	10000	10.1	36.5	10000	7.45	28.0

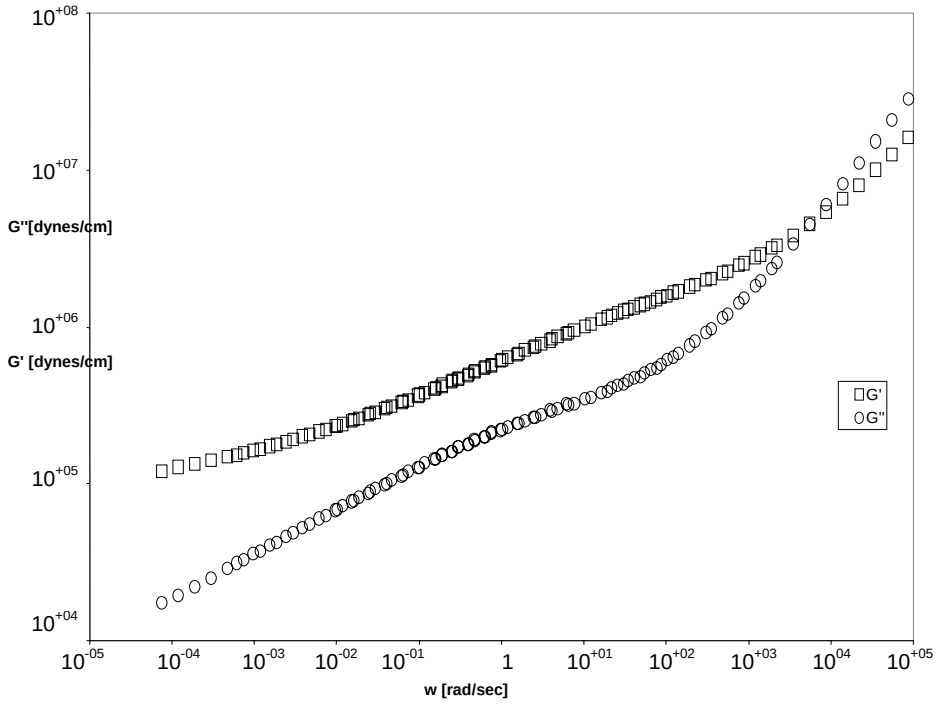

Figure 8.8. Master Curve of MMA-BA copolymer obtained from loss modulus and storage modulus as a function of $\omega(rad/s)$, measured at different temperatures.

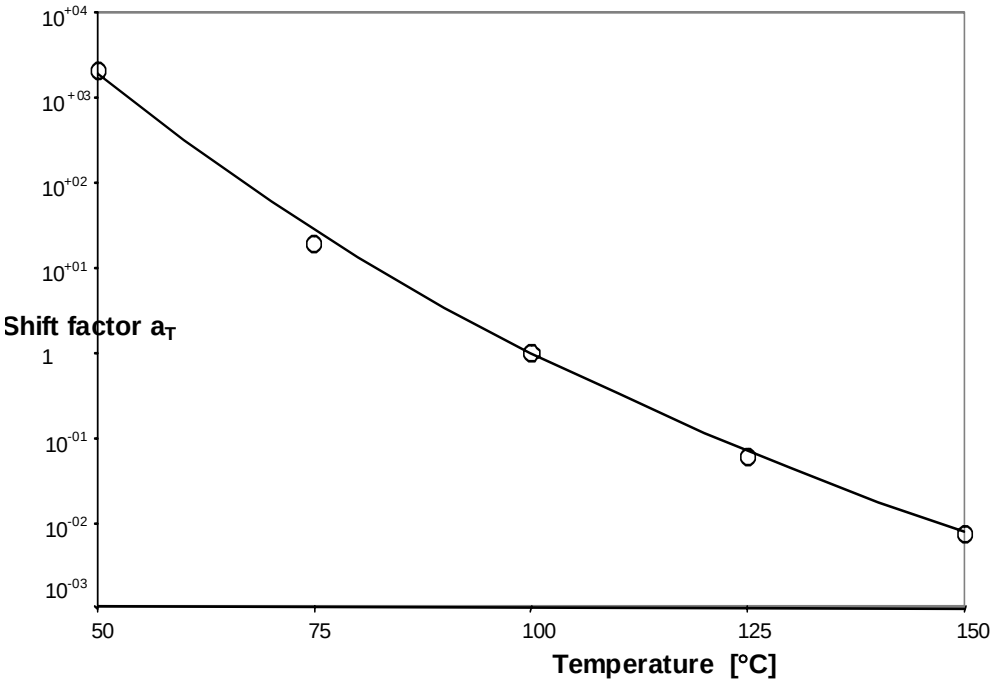

Figure 8.9. The change of shift factor of MMA-BA copolymer with respect to temperature

8.3. Diffusion and Equilibrium Studies

8.3.1. Determination of Diffusion Coefficients of MMA in MMA-BA Copolymer

In this study the diffusivity of MMA in MMA-BA copolymer was measured at 40, 50, and 60°C by using magnetic suspension balance. At the beginning of each new measurement, polymer film was kept in measuring chamber at a certain column temperature under vacuum until the balance reading becomes stable which usually took about 1 day. Meanwhile, the room temperature was maintained constant at 20°C, since the balance reading is affected by the change in room temparature. The minimum and maximum temperature of MMA vapor sent to the column were selected as 23°C and 5°C below the column temperature, respectively. The temperature interval between each set of experiments was kept as small as 3°C. Vapor pressure of MMA was followed by the pressure transducer and observed as constant throughout the experiment. Experimental vapor pressures were found to be in good agreement with those calculated from a correlation given in DICAPS database (Daubert and Danner, 1994). The change in weight of the polymer film and the temperature inside the column were recorded by the computer for every 5 seconds. Before further analysis, data were corrected for buoyancy effect. Normalized mass uptakes of polymer sample $\frac{M_t - M_0}{M_\infty - M_0}$, at each set of the experiments were drawn against the square root of time $\sqrt{t}$, and the results are shown in Figures 8.10 through 8.12. The initial portion of the curves in these figures was linear, thus, Equation 3.7 with the thickness of the sample at the beginning of each set of experiment was used to calculate the diffusivities. Full uptake curves were generated from Equation 3.6 by incorporating these diffusivities and they were compared with the experimental curves. For all cases, deviation between the experimental and theoretical curves was observed. Thus, the diffusivities were recalculated from Equation 3.6 by minimizing the sum of square of the difference between the experimental and theoretical values for the entire sorption curve. As shown in Figures 8.10 through 8.12, theoretical uptake curves appropriately fit the experimental ones with slight deviation in a few cases. Another observation is that all curves are concave with respect to the $\sqrt{t}$ axis. Thus, this condition along with the linearity of the curves in the initial region suggest that sorption kinetics of MMA in MMA-BA copolymer may follow Fickian sorption. Sorption kinetics will be investigated further in the next section.

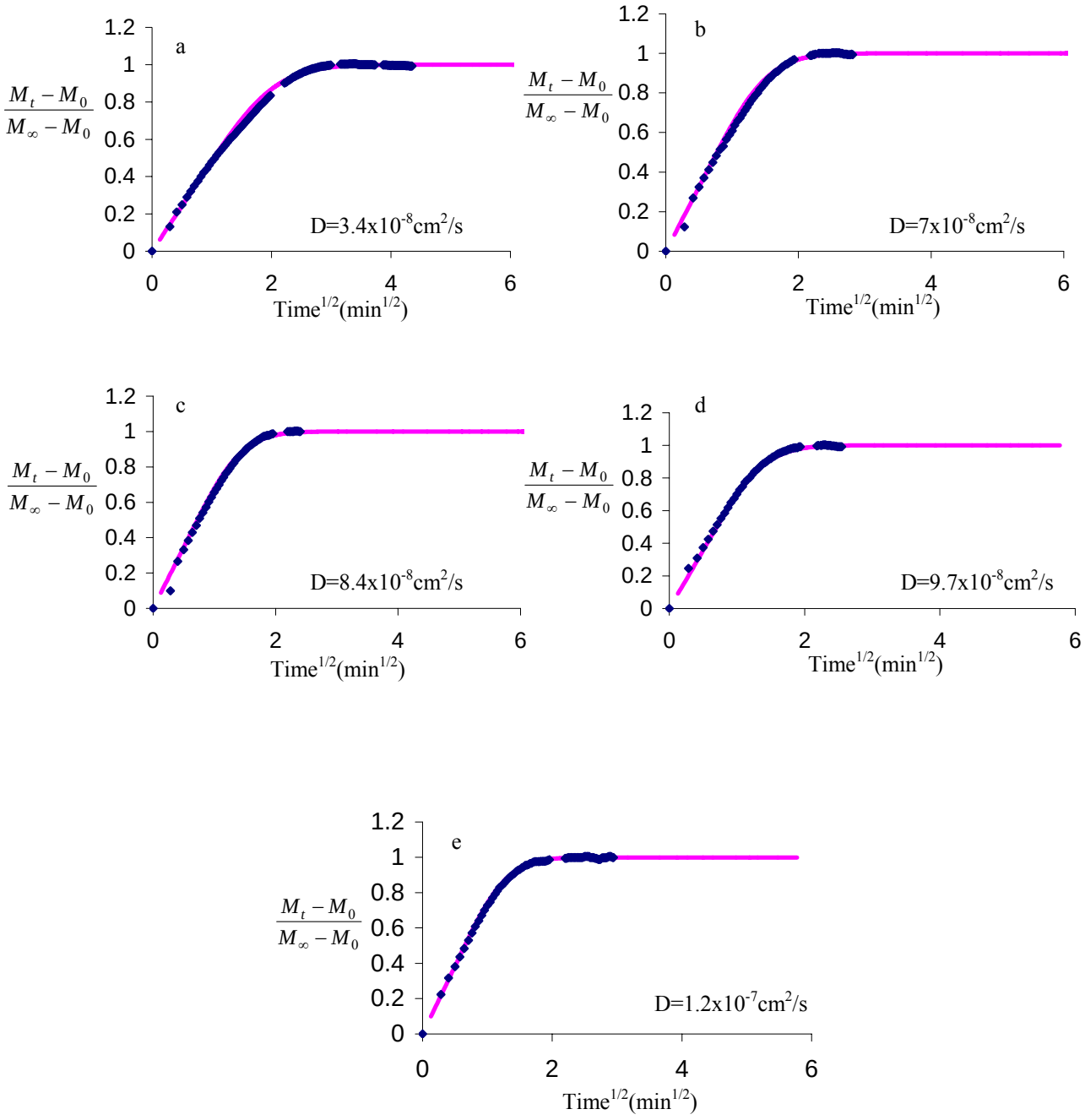

Figure 8.10. Normalized mass uptakes, for the diffusion of MMA into MMA-BA copolymer at 40°C. The solid line represents the theoretical Fickian curve and the symbol represents the experimental sorption curve. Solvent vapor pressures: a) 49.6 mbar, b) 56.6 mbar, c) 67.9 mbar, d) 77.6 mbar, e) 88.9 mbar.

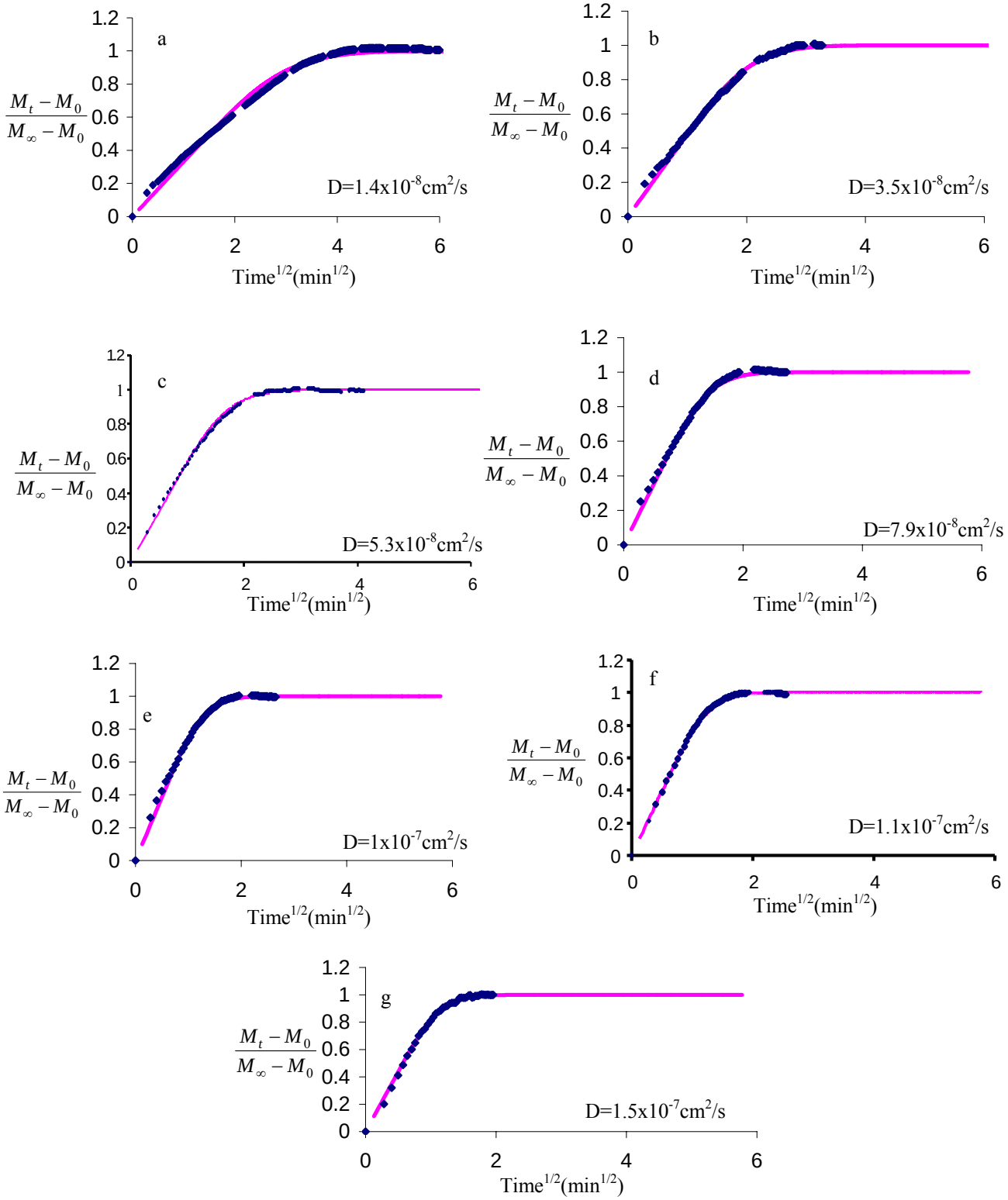

Figure 8.11. Normalized mass uptakes, for the diffusion of MMA into MMA-BA copolymer at 50°C. The solid line represents the theoretical Fickian curve and the symbol represents the experimental sorption curve. Solvent vapor pressures: a) 47.2 mbar, b) 55.5 mbar, c) 63.7 mbar, d) 75.8 mbar, e) 87.2 mbar, f) 104.7 mbar, g) 130.2 mbar.

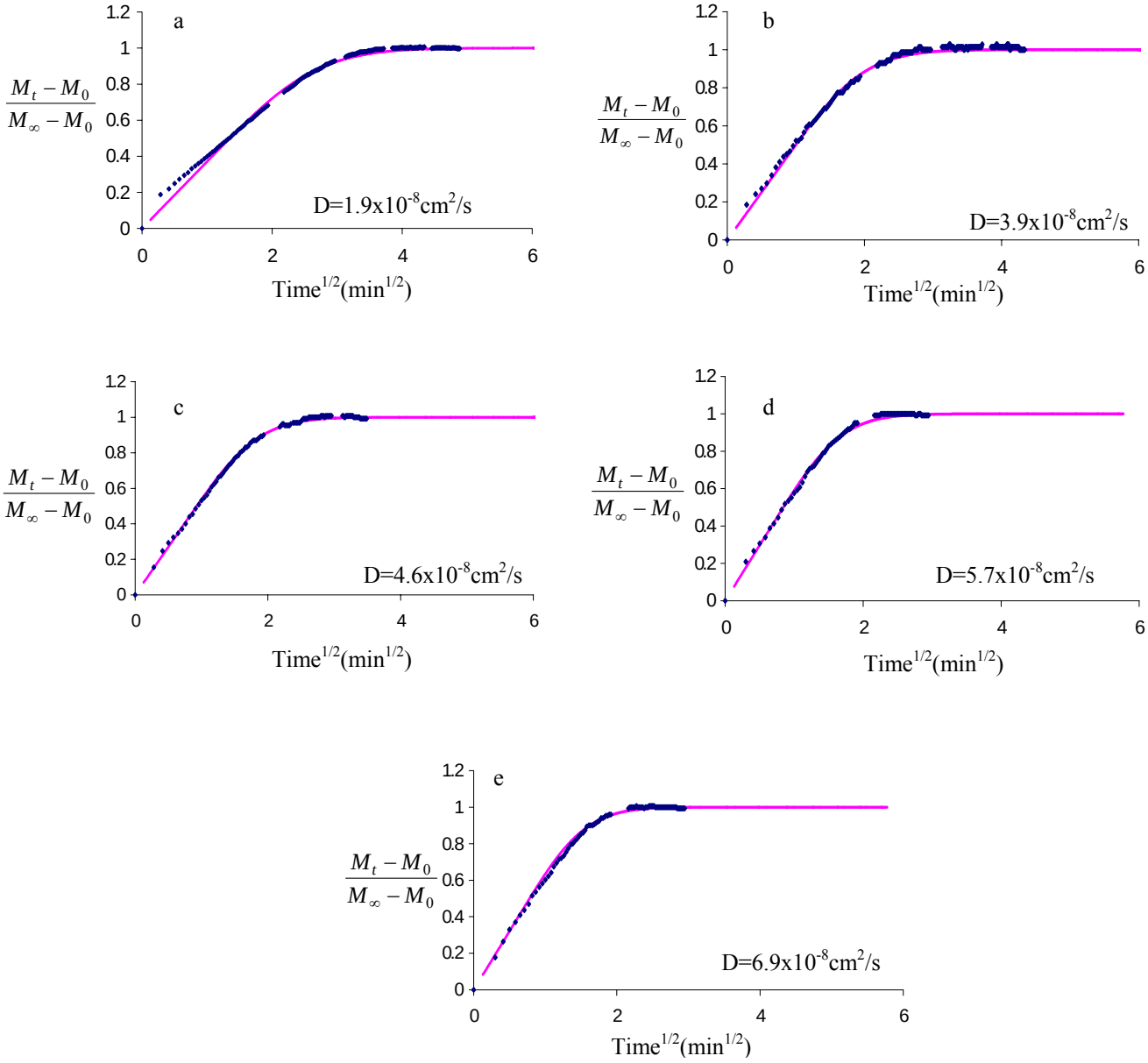

Figure 8.12. Normalized mass uptakes, for the diffusion of MMA into MMA-BA copolymer at 60°C. The solid line represents the theoretical Fickian curve and the symbol represents the experimental sorption curve. Solvent vapor pressures: a) 44.8 mbar, b) 52.4 mbar, c) 63.7 mbar, d) 74.1 mbar, e) 85.4 mbar.

The diffusivities of MMA in MMA-BA copolymer calculated for each set of experiment are listed in Tables 8.3 through 8.5. Included in these tables are initial thicknesses of the sample, initial, equilibrium, and average weight fraction of MMA and initial and final pressures of MMA recorded for each experimental run. The diffusivities reported in these

tables correspond to the average weight fraction of MMA calculated by Equation 8.3 (Hong et al., 1998).

$$\omega_{average} = \omega_{initial} + 0.7\left(\omega_{equilibrium} - \omega_{initial}\right) \tag{8.3}$$

In the calculation of the diffusivities average thickness of the polymer sample ($L_{average} = \frac{L_{initial} + L_{equilibrium}}{2}$) was used. The thickness at the beginning ($L_{initial}$) and at the end of each intermediate experimental step was calculated using following equation.

$$L = \frac{msample\left[\omega_1 \hat{V}_1 + \omega_2 \hat{V}_2\right]}{A} \tag{8.4}$$

Table 8.3. Experimental parameters used to generate mass uptake curves in Figure 8.10.

Temperature (°C)	Pressure(mbar)		ω_{MMA}			thickness (cm)	Dx10^8 (cm^2/s)
	initial	final	initial	equilibrium	average		
40	0.000	49.6	0.000	0.0964	0.06748	0.00643	3.4
	49.6	56.6	0.0964	0.121	0.11362	0.00712	7
	56.6	67.9	0.121	0.155	0.1448	0.00733	8.4
	67.9	77.6	0.155	0.18	0.1725	0.00762	9.7
	77.6	88.9	0.18	0.2063	0.19841	0.00787	12

Table 8.4. Experimental parameters used to generate mass uptake curves in Figure 8.11.

Temperature (°C)	Pressure(psi)		ω_{MMA}			thickness (cm)	Dx10^8 (cm^2/s)
	initial	final	initial	equilibrium	average		
50	0.000	47.2	0.000	0.0629	0.04403	0.00633	1.4
	47.2	55.5	0.0629	0.0755	0.07172	0.00682	3.5
	55.5	63.7	0.0755	0.088	0.08425	0.00693	5.3
	63.7	75.8	0.088	0.107	0.1013	0.00704	7.9
	75.8	87.2	0.107	0.126	0.1203	0.00721	10.0
	87.2	104.7	0.126	0.152	0.1442	0.00738	11.0
	104.7	130.2	0.152	0.1889	0.17783	0.00764	15.0

Table 8.5. Experimental parameters used to generate mass uptake curves in Figure 8.12.

Temperature (°C)	Pressure(psi)		ω_{MMA}			thickness (cm)	Dx10^8 (cm^2/s)
	Initial	final	initial	equilibrium	average		
60	0.000	44.8	0.000	0.0456	0.03192	0.0065	1.9
	44.8	52.4	0.0456	0.053	0.05078	0.00686	3.9
	52.4	63.7	0.053	0.066	0.0621	0.00692	4.6
	63.7	74.1	0.066	0.0785	0.07475	0.00703	5.7
	74.1	85.4	0.0785	0.0931	0.08872	0.00714	6.9

8.3.2. Determination of Kinetic Behavior of MMA in MMA-BA Copolymer

Figures 8.10 through 8.12 indicated that the initial stages of the sorption curves are linear and the curves always concave with respect to the $\sqrt{t}$ axis. These two conditions are required to classify the sorption process as Fickian. In addition, the sorption curves for all values of the film thickness L should form a single curve when plotted as $\frac{M_t - M_0}{M_\infty - M_0}$ vs $\sqrt{t}/L$ for fixed initial and final penetrant concentrations. In order to check validity of the third condition, sorption measurements of MMA were repeated at column temperatures of 40C° and 60 C° using different film thicknesses. Figures 8.13 and 8.14 show that uptake curves obtained at different film thicknesses coincide with each other when $\frac{M_t - M_0}{M_\infty - M_0}$ is plotted against normalized time scale, $\sqrt{t}/L$. The comparisons of the diffusion coefficients measured at different film thicknesses are given in Table 8.6. The results in Figures 8.10 through 8.14 indicate that the sorption kinetic of MMA in MMA-BA copolymer is categorized as Fickian sorption. It was shown that the diffusion coefficients obtained from sorption or desorption experiments are the same when the sorption process behaves as Fickian (Crank and Park, 1968; Wel and Adan, 1999). Based on this observation, the diffusivities obtained from absorption experiments were used in modeling the emission of monomers into air. This will be illustrated in section 8.5.

Table 8.6. Comparison of the diffusion coefficients of MMA in MMA-BA copolymer measured with different film thicknesses

Tcolumn (C°)	Tsolvent (C°)	Initial film thickness (μm)	Diffusion Coefficient x10^8(cm^2/s)	Initial film thickness (μm)	Diffusion Coefficient x10^8 (cm^2/s)
40	30 C° 33 C° 36 C°	65	8.4 9.7 12.0	50	6.7 9.0 11.2
60	30 C° 36 C°	65	4.6 6.9	80	4.1 5.4

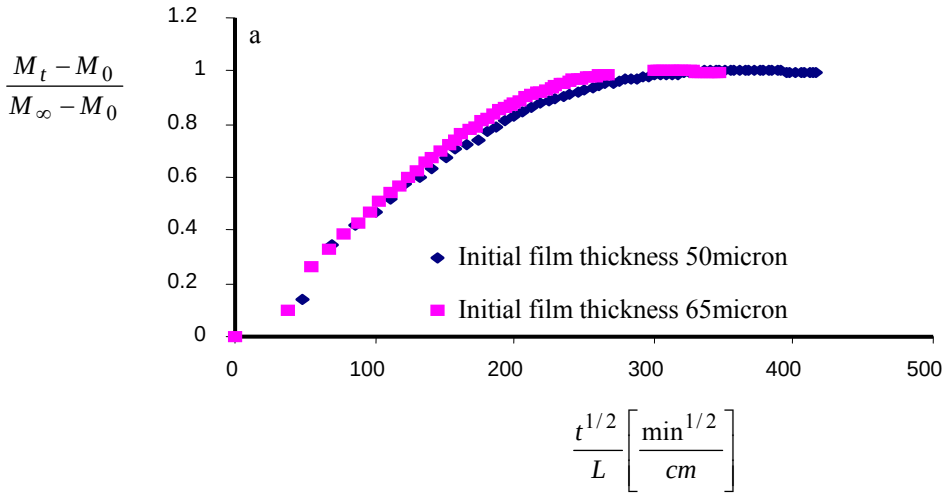

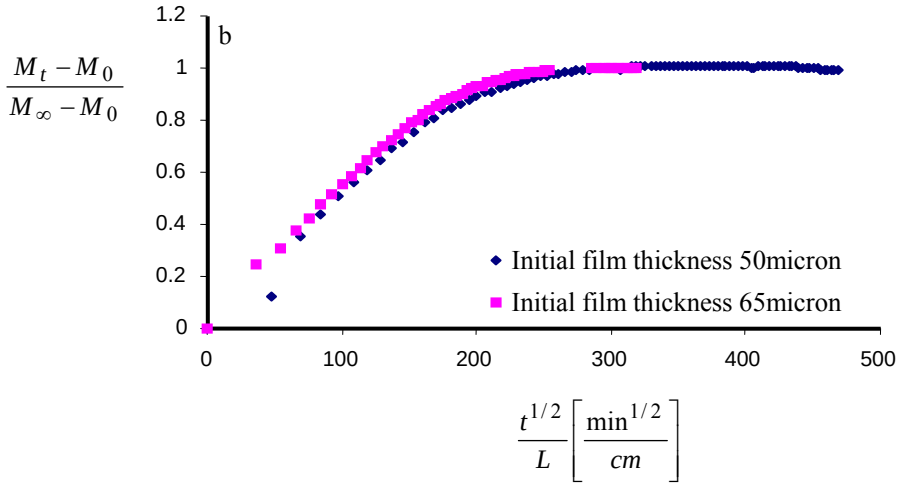

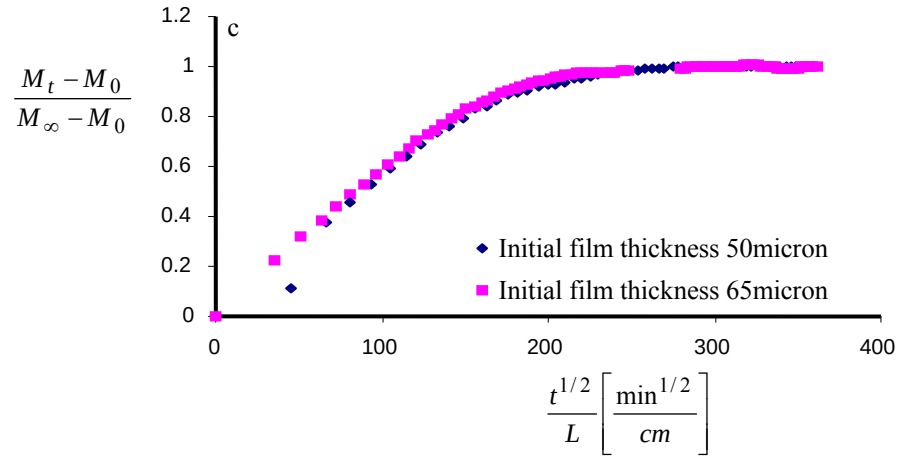

Figure 8.13. Comparison of normalized mass uptake curves for the diffusion of MMA into MMA-BA copolymer, having thicknesses of 50 and 65μm. The column temperature is 40 C° and the solvent pressures are: a) 63.7 mbar, b) 74.1 mbar, c) 85.4mbar

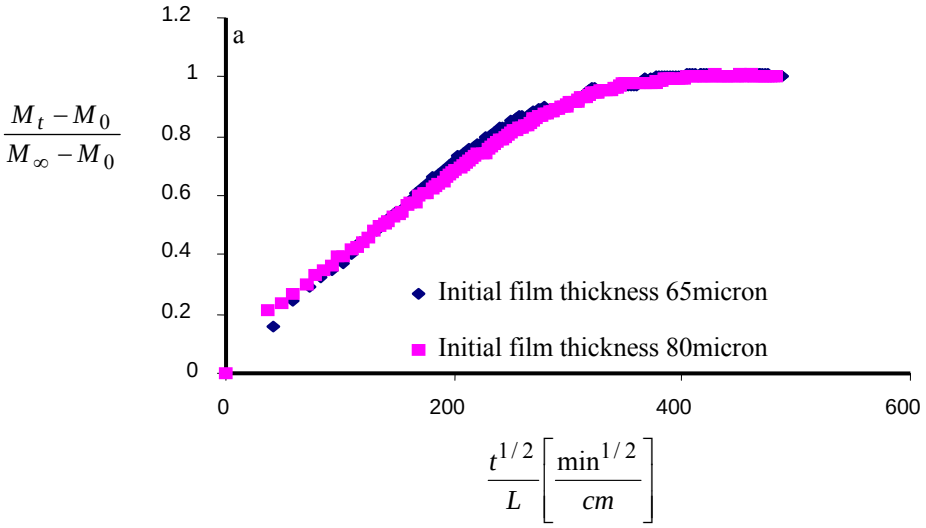

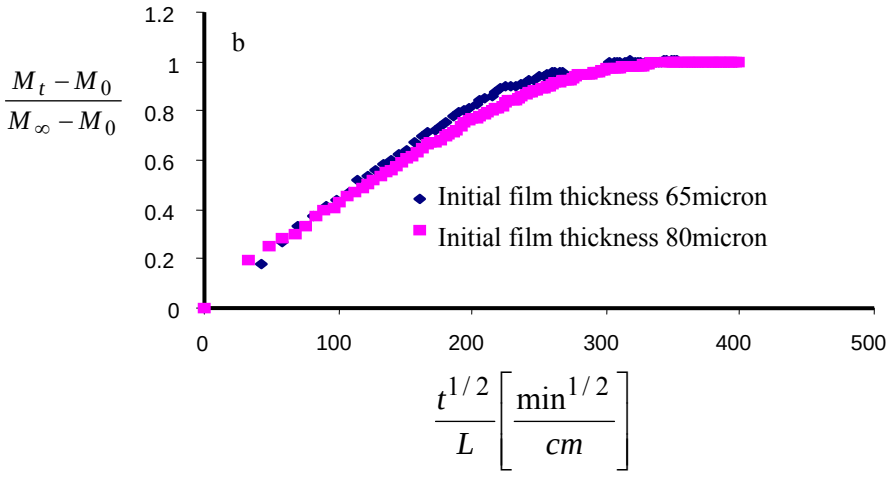

Figure 8.14. Comparison of normalized mass uptake curves for the diffusion of MMA into MMA-BA copolymer, having thicknesses of 65 and 80μm. The column temperature is 60 C° and the solvent pressures are: a) 63.7 mbar , b) 85.4 mbar.

8.3.3. Equilibrium Isotherms

Sorption isotherm of a solvent in a polymer is usually plotted as activity of the solvent in the vapour phase against volume fraction of the solvent in the polymer. By assuming that the solvent vapor is ideal, activity was calculated from the ratio of the saturation vapour pressure of the solvent at the solvent temperature and the column temperature, respectively as given below.

$$Activity = \frac{P_1^{O}(T_{penetrant})}{P_1^{O}(T_{column})} \tag{8.4}$$

From the experimental measurements, solubility of MMA in MMA-BA copolymer at the column temperature of 40, 50, and 60°C were determined and the results are given in Table 8.7.

Table 8.7. Sorption isotherms of MMA in MMA-BA copolymer measured at the column temperatures of 40, 50, and 60°C.

T (^{o}C)	Volume Fraction of MMA	Activity
40	0.109	0.482
	0.137	0.549
	0.174	0.659
	0.202	0.754
	0.23	0.864
50	0.072	0.307
	0.086	0.361
	0.1	0.415
	0.121	0.493
	0.142	0.567
	0.171	0.682
	0.211	0.848
60	0.052	0.177
	0.061	0.207
	0.076	0.252
	0.089	0.293
	0.106	0.338

8.4. Modeling of Diffusion and Equilibrium Studies

8.4.1. Correlation and Prediction of Diffusion Coefficients

In this study, diffusivities were correlated with Vrentas and Duda free volume theory. The unknown parameters in the theory described by Equation 2.1 are D_0^* and ξ. To obtain these two parameters, the diffusivity data collected at 40°C were fitted to Equation 2.1 and following objective function was minimized using solver tool in Excel.

$$\min \sum_{i=1}^{Ndata} \left(\ln D_{experimental} - \ln D_{theoretical} \right)^2 \qquad (8.5)$$

Regressed parameters, D_0^* and ξ, along with the other free volume parameters are listed in Table 8.8.

Table 8.8. Free volume parameters of MMA and MMA-BA copolymer

Parameter		**MMA/MMA-BA**
K_{11}/γ	(cm^3/g.K)	0.002616
K_{12}/γ	(cm^3/g.K)	0.00013
K_{21}-T_{g1}	(K)	-120.2
K_{22}-T_{g2}	(K)	-81.2
$\hat{V}_1^*$	(cm^3/g)	0.871
$\hat{V}_2^*$	(cm^3/g)	0.83
D_o^*	(cm^2/s)	5.19×10^{-6}
ζ		0.3042
χ		0.726

Figure 8.15 shows that diffusivities calculated from Equation 2.1 using the parameters in Table 8.8 are in excellent agreement with the experimental ones. This agreement indicates that Vrentas and Duda free volume theory can correlate the diffusion behavior of MMA in MMA-BA copolymer. The predictive capability of the theory was tested using experimental diffusivity data measured at the column temperatures of 50°C and 60°C. Predictions are compared to experimental data as shown in Figures 8.16 and 8.17. Diffusion coefficients were predicted using the parameters listed in Table 8.8 and are in good agreement at 50°C and in excellent agreement at 60°C. The results in Figures 8.15 through 8.17 indicate that correlation obtained from Vrentas and Duda free volume theory can be accurately used to predict diffusivity of MMA in MMA-BA copolymer.

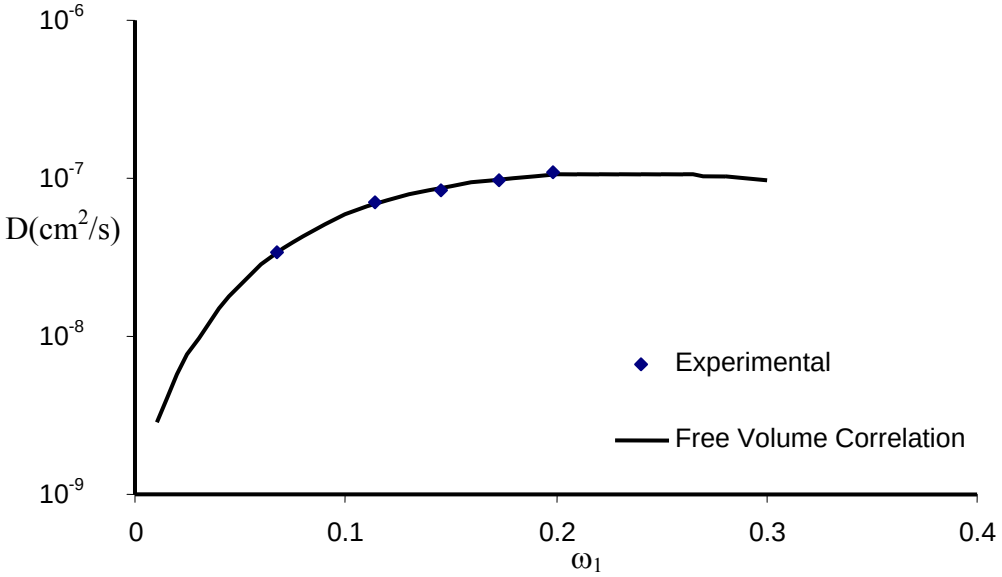

Figure 8.15. Experimental and correlated diffusivities with respect to weight fraction of MMA in MMA-BA copolymer at 40°C.

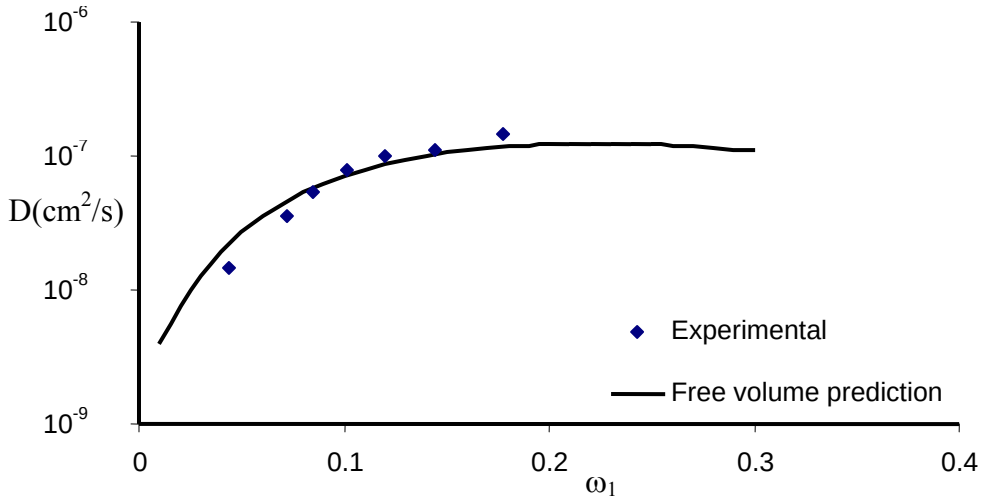

Figure 8.16. Experimental and predicted diffusivities with respect to weight fraction of MMA in MMA-BA copolymer at 50°C.

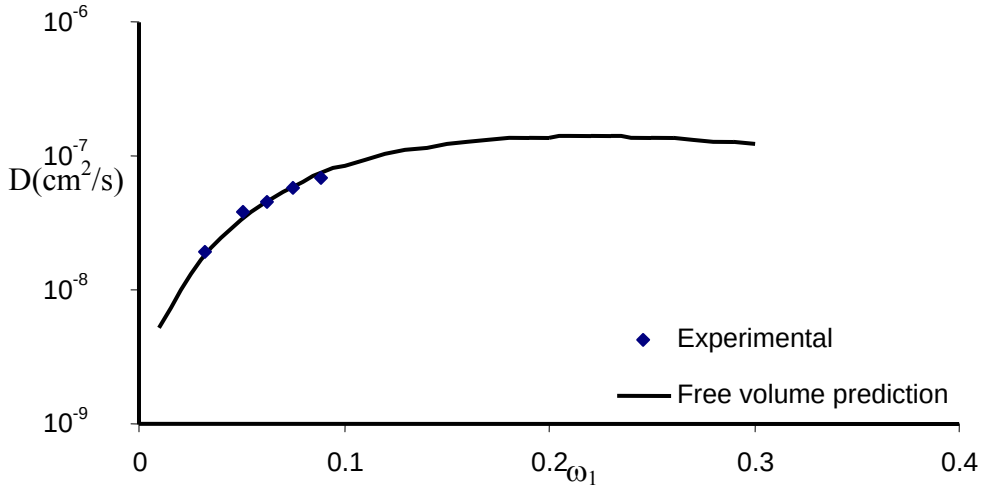

Figure 8.17. Experimental and predicted diffusivities with respect to weight fraction of MMA in MMA-BA copolymer at 60°C.

8.4.2. Modeling of the Equilibrium Isotherm

Thermodynamic behavior and sorption isotherm for many polymer-solvent systems were well defined by Flory-Huggins theory (1953). This theory was also utilized in this study to model the equilibrium isotherm. For this purpose, first the interaction parameter, χ, between the polymer and the monomer was determined using the experimental sorption isotherms at the column temperatures of 40 and 50°C. By minimizing following objective function

$$\min \sum_{i=1}^{Ndata} \left(\ln a_{experimental} - \ln a_{theoretical} \right)^2 \qquad (8.6.)$$

the Flory Huggins interaction parameter between MMA and MMA-BA copolymer was calculated as 0.726. The interaction parameter of MMA greater than 0.5 indicates that MMA is not a good solvent for MMA-BA copolymer. This situation has been observed experimentally. Small piece of MMA-BA film was placed in MMA and the solution was continuously stirred at 40°C for 3 days. At the end of this period, pieces of films still not dissolved in MMA were observed.

Figure 8.18 compares experimental activities with the prediction from the Flory Huggins theory. The theory describes the sorption behavior of MMA in MMA-BA copolymer satisfactorily. Maximum solubility of MMA in the copolymer was calculated as 53% by volume.

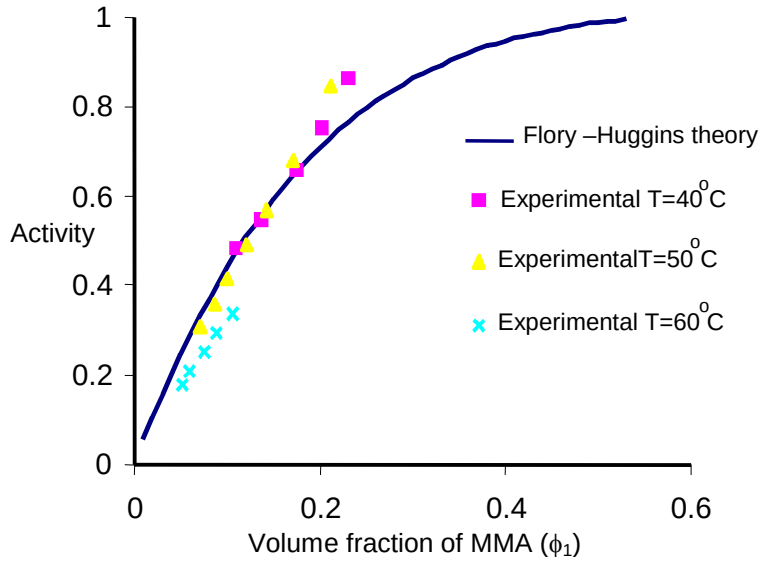

Figure 8.18. Sorption isotherm of MMA in MMA-BA system.

8.5. Determination of MMA Concentration in Air

MMA concentration in air under various conditions was determined by solving coupled nonlinear and ordinary differential equations (Equations 4.1 through 4.8). The solution was performed with finite difference approximation. According to the model, emission characteristics of the volatile organic compound (VOC) are initially determined by external conditions such as mass transfer coefficient, air temperature and activity of the volatile compound. Once the external mass transfer resistance is no longer limiting, the key issue in the prediction is the calculation of diffusivity of VOC in the polymer. Diffusivities and activities required for the solution of model equations were calculated using the correlations obtained from experimental measurements. In the analysis, it was assumed that diffusivity of MMA measured in the binder material of the paint can be used to represent diffusion characteristics in the paint.

Concentration of MMA in the copolymer was measured as 110 ppm by the supplier company, Organic Kimya A.Ş. This value was taken as a base value for the initial simulations. Under different conditions, the concentrations of MMA in a room having a volume of 75m^3 and in the polymer were calculated and the results are shown below.

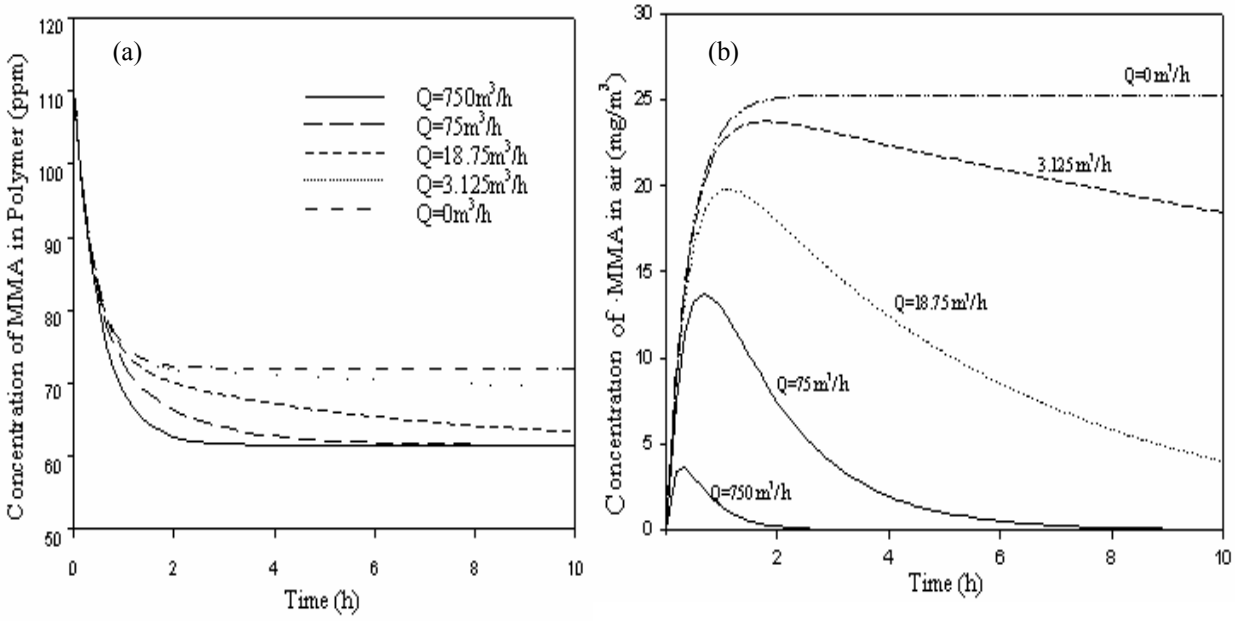

Figure 8.19. Effect of air exchange rate on a) the concentration of MMA in the polymer b) the concentration of MMA in air. (V=75 m^3, ρ_{1o}=110 ppm, k_1^G=1.57 m/h, T=23°C).

Figure 8.19 indicates that increasing air exchange rate reduces the concentration of MMA in air. Initially MMA accumulates in air, then its level starts decreasing since the rate of removal of MMA through ventilation becomes larger than the rate of emission from building material into air. This situation also causes to observe the same concentration of MMA in the polymer during the first few hours of emission. However at later stages, the concentration of MMA in the polymer decreases as the air exchange rate is increased. This is due to the fact that during this period the rate of evaporation of MMA increases with the decrease in MMA level in air. At much longer times (at the end of sixth day) the concentration of MMA in the polymer is almost the same for all air exchange rates since within this period, the rate of emission is controlled by diffusion inside the polymer. The effect of air temperature on the concentrations of MMA in the polymer and in air is illustrated in Figure 9.20. Increasing air temperature from 23°C to 27°C decreases the concentration of

MMA in the polymer since both the diffusivity and the activity of MMA increase as the temperature increases.

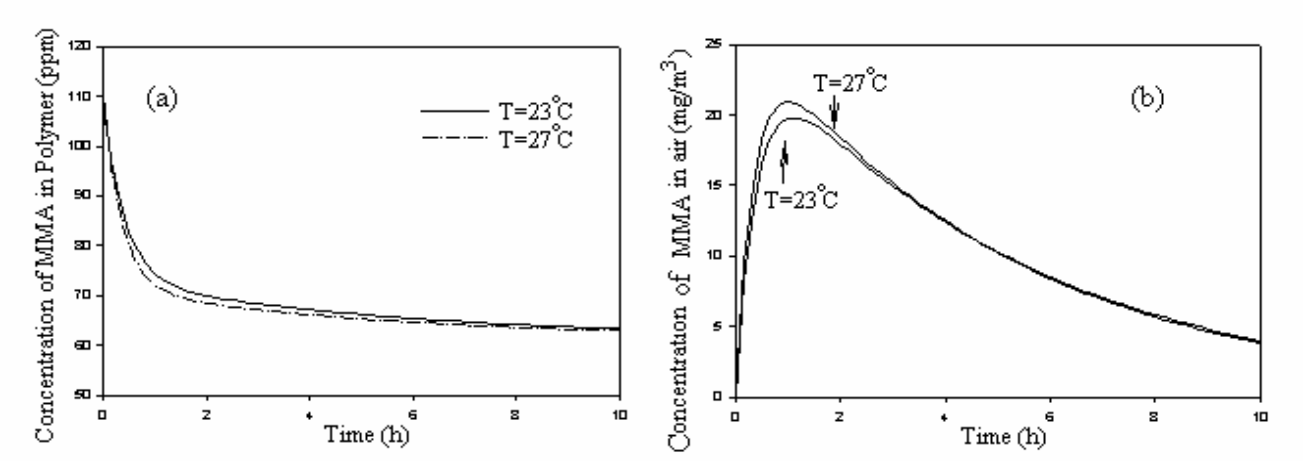

Figure 8.20. Effect of air temperature on a) the concentration of MMA in the polymer b)the concentration of MMA in air (V=75 m^3, ρ_{1o}=110 ppm, k_1^G=1.57 m/h Q=18.75 m^3/h).

More emission of MMA with an increase in air temperature causes higher maximum concentration of MMA in air since air exchange rate is the same in both cases. Figure 8.21 shows the effect of air circulation rate in the room, i.e., air velocity on the level of MMA.

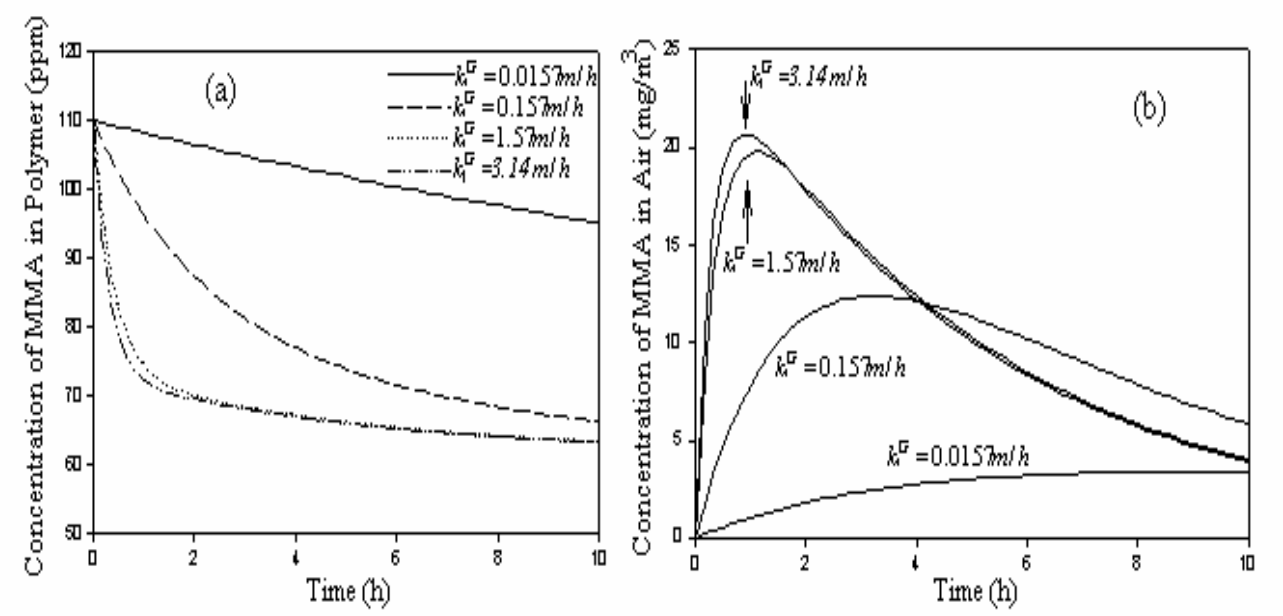

Figure 8.21. Effect of air velocity on a) the concentration of MMA in the polymer b)the concentration of MMA in air (V=75 m^3, ρ_{1o}=110 ppm, Q=18.75 m^3/h, T=23^{o}C).

At low air velocities which correspond to the low mass transfer coefficients, the concentration of MMA both in air and in the polymer is very sensitive to changes in air velocity since the external mass transfer resistance controls the rate of emission of MMA. Increasing air velocity causes higher MMA concentrations in air especially during the initial period of emission. At high mass transfer coefficients and at the end of long period, the concentration of MMA in the polymer becomes independent air velocity, since within this period the rate of emission is controlled by diffusion of MMA in the polymer. If initial concentration of MMA increases from 110 ppm to 400 ppm, then both MMA level in air and the residual amount of MMA in the polymer at the end of 10 hours increase significantly as shown in Figure 8.22.

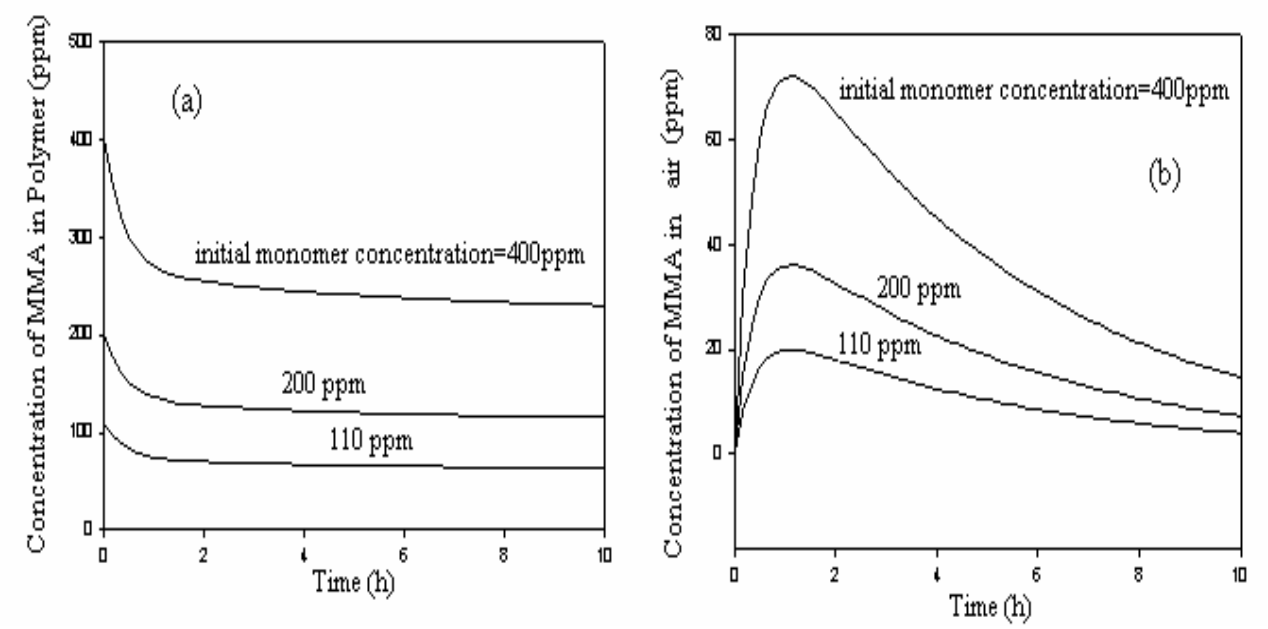

Figure 8.22. Effect of initial MMA concentration on a) the concentration of MMA in the polymer b) the concentration of MMA in air (V=75 m^3, k_1^G=1.57m/h, Q=18.75 m^3/h, T=23^oC).

United States Environmental Protection Agency (USEPA) has reported that MMA does not have carcinogenic effect. However, respiratory effects have been reported in humans following short-term and long-term inhalation exposures. Respiratory symptoms observed include chest tightness, coughing, wheezing and reduced peak flow. Symptoms such as headache, dizziness, difficulty in concentrating and tiredness have also been reported. EPA has reported odor threshold of MMA as 0.2 mg/m^3 and recommended exposure limit for an 8 or 10 hour time-weighted- average exposure as 410mg/m^3. To calculate 8-hour time weighted

average concentrations for various conditions reported in Figures 8.19 through 8.22, following equation was used:

$$\overline{C}_{air} = \frac{1}{8} \int_{t=0}^{t=8hours} C_{air}(t)dt \qquad (8.7)$$

Table 8.9. 8 hour time-weighted average concentration of MMA in air

Parameter	**Value**	$\overline{C}_{air}$ **(mg/m^3)**	**Other Values**
Air exchange rate	Q=750 m^3/h	0.414	ρ_{1o}=110 ppm
	Q=75 m^3/h	4.028	k_1^G=1.57 m/h
	Q=18.75 m^3/h	12.31	T =23 ^{o}C
	Q=3.125 m^3/h	21.14	
	Q=0 m^3/h	23.99	
Air temperature	T=23 ^{o}C	12.31	ρ_{1o}=110 ppm
	T=27 ^{o}C	12.59	k_1^G=1.57 m/h
			Q =18.75 m^3/h
Air velocity	k_1^G=0.0157 m/h	2.40	ρ_{1o}=110 ppm
	k_1^G=0.157 m/h	9.88	Q =18.75 m^3/h
	k_1^G=1.57 m/h	12.31	T =23 ^{o}C
	k_1^G=3.14 m/h	12.42	
Initial monomer Concentration in the polymer	ρ_{1o}=110 ppm	12.31	k_1^G=1.57 m/h
	ρ_{1o}=200 ppm	22.38	T =23 ^{o}C
	ρ_{1o}=400 ppm	44.78	Q =18.75 m^3/h

The integral in Equation 8.7 was calculated numerically using Simpson's rule and 8-hour time weighted average concentrations are given in Table 8.9. All average concentrations corresponding to different conditions are below the recommended exposure limit but above the odor threshold value. Thus, complaint about odour will increase especially with increasing initial monomer concentration in the polymer.

CONCLUSIONS AND FUTURE STUDIES

In this study, solubility and diffusion coefficients of methylmethacrylate (MMA) in methylmethacrylate-co-n-butylacrylate (MMA-BA) copolymer were measured at temperatures of 40°C, 50°C and 60°C by performing gravimetric sorption experiments using a new type of apparatus called magnetic suspension balance. Measurements have shown that diffusivity of MMA in the copolymer varies in the range of $1x10^{-8}$-$1x10^{-7}$ cm^2/s as the weight fraction of MMA increased from 0.03 to 0.2.

The characterization results have shown that the MMA-BA copolymer has glass transition temperature of 40.9°C, degradation temperature of 300°C, and has a composition of 19.7% (by weight) MMA and 80.3% BA monomers. It was observed from the SEM pictures that the polymer films prepared are nonporous and homogenous.

The results of the sorption experiments were normalized and presented by plots of $\frac{M_t - M_0}{M_\infty - M_0}$ as a function of $\sqrt{t}$. It was observed that in the initial stages of the sorption process, the sorption curves are linear and are always concave with respect to $\sqrt{t}$ axis above the linear portion. In addition, the sorption curves obtained with different film thicknesses formed a single curve when plotted as $\frac{M_t - M_0}{M_\infty - M_0}$ vs. normalized time scale $\frac{\sqrt{t}}{L}$ for fixed initial and final penetrant concentrations. Based on these observations, sorption kinetics of MMA in MMA-BA copolymer was classified as Fickian type. Good agreement between experimental and theoretical sorption curves indicated that diffusivities were determined accurately.

Equilibrium solubility data were accurately modeled by Flory Huggins theory. The Flory Huggins interaction parameter was determined as 0.726, which indicated that MMA is not a good solvent for MMA-BA copolymer. According to the prediction of Flory Huggins theory, maximum amount of MMA which can be absorbed in the copolymer is 53% by volume.

Experimental diffusivities were correlated by Vrentas and Duda free volume theory to obtain an expression that describes diffusivity of MMA in MMA-BA copolymer as a function of temperature and concentration. Based on the comparison

between the experimental and predicted diffusivities, the correlative and predictive ability of the Vrentas and Duda theory were found to be satisfactory.

The correlation can be practically used either in the design and optimization of the devolatilization process or in determining the emission characteristics of MMA from the copolymer. In most cases, devolatilization process is operated at elevated temperatures where measurements of diffusivity of MMA are not available due to the risk of polymerization of the monomer at high temperatures. Thus, the correlation obtained in this study becomes a practical tool to predict diffusivities at the devolatilization processing conditions.

The mathematical model derived by Alsoy (1998) for predicting the drying rate of solvent coated polymeric films was extended to determine the emission characteristics of the volatile organic compounds (VOC) from the building materials such as paint. The results have shown that the rate of emission of MMA is controlled both by diffusion in the copolymer and the rate of evaporation from the surface. The rate of emission at the initial stages was found to increase with air temperature and velocity and the air exchange rate. However, at long times, the residual amount of MMA, thus, the rate of emission became independent of these parameters since, during that period, the emission is controlled by diffusion in the polymer. The model shown in this study is general and can be applicable to large number of systems if two key model parameters, diffusivity and solubility of VOC, are available. This model can serve as a practical tool for choosing environmentally friendly building materials and an appropriate ventilation scheme, which would lower VOC concentration in air. Furthermore, model predictions can be used to find the relationship between the emission rate of VOC and the conditions in the room such as air exchange rate, air temperature and velocity.

Future work should involve the measurement of diffusivity and solubility of other monomer of the copolymer, butylacrylate. In addition, the influence of other paint ingredients on the diffusion behavior of the monomers should be investigated by performing experiments on the paint films.

REFERENCES

1. "Anticipation of Anomalous Effects in Differential Sorption Experiment" Vrentas J.S., Vrentas C.M., Huang W.J., November, 1996
   394, (1993).
2. Alsoy, S., "Modeling of Polymer Drying and Devolatilization Processes," PhD. Thesis, The Pennsylvania State Univ., University Park (1998)
3. Axley, J.W., Indoor Air, 2, 47-171, (1991).
4. Cohen M.H., Turnbull D., J. Chem. Phys., 31, 1164, (1959)
5. Crank J., "The Mathematics of Diffusion", Second ed., Oxford University Press, Oxford, 1975, p.238-244
6. Crank, J., Park, G.S., "Diffusion in Polymers", Academic Press, New York, (1968).
7. Daubert, T.E., and R.P. Danner, Physical and Thermodynamic Properties of Pure Compounds: Data Compilation, Taylor & Francis, New York, (1994).
8. Duda,J.L."Devolatilization of Polymers", Biesenberger,J.A. Ed.,Section III, Munih, (1983)
9. Duda,J.L.; Vrentas,J.S.;Ju,S.T.;Liu,S.T. AIChE, (in press)
10. Duda,J.L.; Vrentas,J.S.;Ju,S.T.;Liu,S.T. AIChE J. Vol.28, March, (1982)
11. Dullien FAL. AIChE J. 18, 62, (1972)
12. Dunn, J.E., Chen, T., Symposium on Modeling Indoor Air Quality and Exposure, Pittspurg, PA, ASTM, Philadelphia, PA, pp. 27-28, April 1992.
13. Dunn, J.E., Atmospheric Environment, 21, 425-430 , (1987).
14. Dunn, J.E., Tichenor, B.A., Atmospheric Environment, 22, 885-894, (1988).
15. Faldi A., Tirell M, Lodge T, von Meerwall E., Macromolecules, 27, 4184-4192, (1994)
16. Fick A., Annln Phys., 170, 59, (1855)
17. Flory P.J., Principles of polymer chemistry , Cornell University Press, Ithaca, New York, (1953)
18. Fujita H., Fortschr.HochPolym.-Forsch., 3, 1, (1961)
19. Griffiths, C.M; Strauch, J.;Monteiro, J.M;Gilbert, G.R., J.Macromolecules, 31, 7835, (1998)

20. Haward, R.N. J.Macro.Sci.Rev.Macromol.Chem., 191,(1970)
21. Hong S.U., Laurer J.H., Zielinski J.M., Samseth J., Smith S.D., Duda J.L., Spontak R.J., Macromolecules, 31, 2174-2184, (1998)
22. J.D.Ferry, "Viscoelastic Properties of Polymers", 2nd ed., Wiley, New York, (1970)
23. Ju,S.T.;Liu,H.T.; Duda,J.L.; Vrentas,J.S., J.Appl.Poly.Sci.,26, 3735, (1981)
24. Kim, Y.M., Harrad, S., Harrison, R.M., Environmental Science and Technology, 35, 997-1004, (2001)
25. Kleinrahm, R., and Wagner, W., J. Chem. Thermodyn., 18, 739, (1986)
26. Kobuchi S., Arai Y., Progress in Polymer Science, 27, (2002), 811-814
27. Little, J.C., Hodgeson, A.T., Ashok, J., Atmospheric Environment, 28, 227-234, (1994).
28. Mamaliga, I., Schabel, W., Kind, M., Chemical Engineering and Processing, Article in press, 1-12, (2003).
29. Matthews, T.G., Hawthorne, A.R., Thomson, C.V., Environmental Science and Technology, 21, 629-634 (1987).
30. McDowell C.C., Coker D. T., Freeman B. D., Review of Scientific Instruments, Vol 69, Number 6, (1998)
31. Meininghaus, R., Salthammer, T., Knöppel, H., Atmospheric Environment, 33, 2395-2401, (1999)
32. Molhave, L., Environment, 15, 65-74, (1989)
33. Pawlisch C.A., Macris A., Laurence R.L., Macromolecules, 20, 1564-1578, (1987)
34. Riddle, E.H., "Monomeric Acrylic Esters," Reinhold Publishing Corp., New York (1954).
35. Saby-Dubreuil A.-C., Guerrier B., Allain C., Johanssmann D., Polymer, 42, 1383-1391, (2001)
36. Sato Y., Takikava T., Takishima S, Masuoka H., J. Supercritical Fluids, 19, (2001), 187-198
37. Tichenor, B.A., Guo, Z., Dunn, J.E., Sparks, L.E., Mason , M.A., Indoor Air I,23-25, (1991).
38. Tonge, M.P; Gilbert, R.G., J. Polymer, 42,1393, (2001)

39. US EPA, Reducing risk: setting priorities and strategies for environmental protection, Science Advisory Board, US Environmental Protection Agency, Washington, DC, (1990).
40. Van Der Wel, G.K., Adan, O.C.G., Progress in Organic Coatings, 37, 1 (1999).
41. Vrentas J.S., Vrentas C.M., J. of Polymer Science, Part B, Polymer Physics, Vol 36, 171-180, (1998)
42. Vrentas J.S., Vrentas C.M., J. of Polymer Science, Part B, Polymer Physics, Vol 39, 1529-1547, (2001)
43. Vrentas J.S., Duda J.L., J. of Polymer Science, Polymer Physics, Vol 15, 441-453, (1977c)
44. Vrentas J.S., Duda J.L.,J. Applied Polymer Science, 21, 1715, (1977d)
45. Vrentas J.S., Duda J.L., Ju S.T., Ni L.-W., Journal of Membrane Science, 18, 161-175, (1984)
46. Vrentas, J.S.; Vrentas, C.M; Faridi, N, Macromolecules, 29, (1996)
47. Vrentas, J.S.; Liu, H.T.;Duda, J.L. , J.Appl..Poly.Sci., 25, (1980)
48. Vrentas, J.S.; Duda, J.L., J.Appl.Poly. Sci., 21, 1715, (1977b)
49. Vrentas, J.S.; Vrentas, C.M. Eur. Poly. J.,34, 797, (1998)
50. Vrentas,J.S.; Duda,J.L. J.Polym.Sci. 15, 403, (1977a)
51. Vrentas,J.S.; Duda,J.L. AIChE J., 25, 1, (1979)
52. Vrentas,J.S.;Jarzebski,C.M.;Duda,J.L. AIChE J., 21, 894, (1975)
53. World Health Organization, Indoor air quality: organic pollutants, Copenagen, WHO reginal office for Europe (EURO Report and Studies, 1111), (1989).
54. Yang, X., Study of building materials emissions and indoor air quality. Ph.D. Thesis, Massachusetts Institute of Technology, (1999).
55. Zielinski, J.M. ve Duda , J.L., AIChE J., 38, 405, (1992).